nature portfolio

Peer Review File

Transcranial optogenetic brain modulator for precise bimodal neuromodulation in multiple brain regions

Corresponding Author: Professor Il-Joo Cho

This file contains all reviewer reports in order by version, followed by all author rebuttals in order by version.

Version 1:

Reviewer comments:

Reviewer #1

(Remarks to the Author)
This article reports a wirelessly operated LED system that can optogenetically activate and inhibit neural activities, when combined with opsins like ReaChR and stGtACR2 as well as blue/green upconversion nanoparticles (UCPs). The red and IR LEDs are mounted on the surface of scalp without implantation, which minimizes the brain tissue damage. Wireless, bimodal neural modulations are successfully demonstrated in a mouse model, in multiple brain regions like M2, SC, mPFC, dmST. The paper is well written and has comprehensive animal studies. However, there are multiple issues that are needed to be addressed before the publication.

Major comments:

1. Thermal Issue: How hot is the LED? These LEDs are operated at a very high power (2.1 V, 0.25 A)? What is the temperature rise during the operation? How will it affect the mouse scalp and brain tissue? Some thermal measurements and simulations should be provided.

2. Power Issue: How long can the battery last? The battery used in the circuit has a capacity of 30 mAh. The LED is operated at 2.1 V, 0.25 A, 50% duty cycle. Based on a simple estimation, the battery can only last for <15 mins if only one LED is on. To operate multiple LEDs, the battery lifetime will be even shorter.

3. Optical Issue: What are the spectral overlap of ReaChR, stGtACR2, red LED, NIR LED, blue and green UCPs? Excitation spectra of opsins (ReaChR and stGtACR2) and emission spectra of light sources (LEDs and UCPs) should be presented together, so we can check their overlaps. It is speculated that when ReaChR and stGtACR2 are co-expressed in the same region, green light would excite both of them.

4. Resolution Issue: What is the spatial resolution for external light stimulation? Optical modeling can be used to evaluate the volume of a brain region that is modulated when light is applied extracranially. The paper claims that its technique has “high spatial resolution”, but it is doubtful. The light distribution will be widespread after passing through the skull. Therefore, its spatial resolution should be inferior to implantable light sources.

5. Viral Expression Issue. In the fluorescence images (Fig. 2b, S11, S12), the viral expressions are not clear at all, and cell bodies cannot be distinguished. It is difficult to tell if the opsin expressions (ReaChR and stGtACR2) are successful. For example, in Fig. 2b, it is impossible to count how many cells are expressed with ReaChR under different injection doses. Also, DAPI staining is suggested to use to label the cell body.

Other minor issues:

6. Fig. S1, please label the intracellular and extracellular regions, and double check the ion flow direction for ReaChR. Should K+ ions flow in or out?

7. Table S1, it is not fair to make such a comparison. For those invasive methods, their advantages are that they can reach very deep tissue. Therefore, it is suggested that at least the stimulation depth should be added in this table.

8. Fig. 3: “p>0.999999999999999” is not a proper usage.

9. Fig, 4: “p<0.000000000000001” is not a proper usage.

10. Line 141, “at 63 mW·mm-2 (2.1 V, 0.25 A)”. How and where to get the power density of 63 mW·mm-2?

11. Line 48, “However, light must be delivered into the target region using an implanted fiber”, not correct. Light can also be delivered using LED or waveguide based implants.

Reviewer #2

(Remarks to the Author)
The manuscript ‘Non-invasive wireless brain modulator for precise bimodal neuromodulation in multiple brain regions’ by Shin et al. report their platform consisting of two-colored LEDs which can be wirelessly driven which can be used as a light source for optogenetics. The genetically modified channelrhodopsins ReaChR and soma targeted GtACR2 are tagged with upconverting nanoparticles (UCNPs) thus the exciting wavelengths are in the red an NIR spectral range. In vivo neuromodulation is performed leading to motion and behavioural control of mice.
I rate the importance of the published work in this subject area as top 30%. Novelty is in the top 50% as well. The scholarly representation needs further work in terms of English language, clarity and specificity of paragraphs. Especially the language should be checked by a native speaker. The methods are mostly testing the hypothesis, but not sufficiently described, both can be improved. I have some major concerns that have to be addressed and further evidence provided before considering this manuscript for publication.
Here are my detailed comments on the manuscript:
1. The authors claim that their technique is non-invasive, however, the genetic modification needs a craniotomy in order to insert the respective ChRs and UCNPs. Thus, it is arguable that the entire technique including the genetic modification is non-invasive. In the process the modulation is performed via transcranial light exposure, which is non-invasive, but only one part of the presented technique. Thus, the wording has to be changed accordingly to not misguide the readers.
2. In the list of NIBS mentioned, tNIRS should be named as well as this is best comparable to the presented work. Reference 10 is a good example for this.
3. In l.63 fiber and micro-LEDs are mentioned as invasive devices. For completeness micro-OLEDs should be added: https://www.nature.com/articles/s41928-023-01013-y
4. In the abstract the authors very repeatedly and excessively use the terms (non-) invasive, and bimodal neurostimulation without giving much insight into the technique. Especially in the abstract the key findings are missing and should be described more precisely.
5. The characterization of the LEDs is entirely missing. There are no spectra shown, no jVP curves. Same holds for the UCNPs absorption. How does the spectral overlap look like, are the red and NIR emission spectra of the LEDs clearly separated? Is there a chance of crosstalk of the modulations? How does the overlap with ReaChR look like? There is only very poor information given on this, mainly just the power and power density, which is insufficient.
6. How is the modulation pattern of 63 mW/mm² (red) and 275.5 mW/mm² (NIR) and 10Hz with ON time of 10ms (10% duty cycle) chosen? How long is the stimulation, always 10min? Are there previous experiments or literature that suggest this pattern? What is the benefit of it? This has to be clarified in the manuscript.
7. The power used is very high. Have the authors checked the heat deposition in the skull and tissue? An increase in 1deg in biological tissue is already thought to be critical for neuronal behaviour, see https://www.nature.com/articles/s41593-019-0422-3 Can the authors comment on this? It would be necessary to perform measurements supported by simulations in order to exclude heat effects.
8. Red and NIR light can be used for neuromodulation without the use of genetically modified ChRs. Photobiomodulation (PBM) in order to increase neuronal activity is a growing field used to treat neurodegenerative diseases, e.g. by transcranial NIRS https://www.frontiersin.org/journals/pharmacology/articles/10.3389/fphar.2022.965788/full
The absorption by the enzyme Cytochrome C oxidase and heat sensitive transmembrane channels is causing the effect of the PBM. This depends strongly on the wavelength (>600nm) and exposure to light (intensity, power…). The control experiments in this publication do most often not account for this possible effect. In the case of spatial resolution determination (since PBM can also increase cFos signal), this should be tested with WT mice. For motion and bahvioral contral WT mice were tested and for this certain experiment this is ok. But in the case of Parkinsonism it should be tested if the motor dysfunction of mice without genetic modification but MPTP injection can be improved by the LED probe itself without the need of optogenetics. This requires further tests.
9. It is not clear if the position of the LED probe in the control experiments mentioned in l. 195 is exactly the same as in the experiment later. Where is it placed? This should be added in a figure.
10. The wording of mind and body control is misleading and should be named into behavioural and motion control instead.
11. The improvement in resolution should be compared to the resolution of the mentioned transcranial techniques, numbers should be provided.

Version 2:

Reviewer comments:

Reviewer #1

(Remarks to the Author)
The authors have addressed all the Reviewers' comments accordingly. I suggest the paper be accepted.

Reviewer #2

(Remarks to the Author)
The authors have thoroughly and thoughtfully addressed my previous comments on their manuscript. The in-depth elaboration on the device's thermal and spectral properties, along with the additional information on control experiments, provides essential and valuable insights into their work and findings. These enhancements strengthen both the experimental setup and analysis, making the experimental approach and the concept of this transcranial LED-based stimulation device clearer and more accessible. Looking forward, an overlap of 60% between blue UCPs and ReaChR may be excessive and could potentially reduce effectiveness when aiming to inhibit neurons through stGtACR2.

There is one remaining concern which should be addressed before the publication:
Line 301: The authors simulate and calculate the optimal distance for LEDs within the device, yet the actual LED spacing on the skull remains unclear. The authors should specify the precise placement for the different experiments (e.g., motion control and behavioral studies), including details on the distances of the LEDs and the accuracy of the placement in order to guarantee reproducibilty.

RESPONSES TO REVIEWER'S COMMENTS FOR NCOMMS-23-12932B

We appreciate the reviewer's careful evaluations and insightful comments on our paper. We have addressed all the comments and feel that the constructive comments were in many ways helpful and significantly improved our manuscript. We have listed each of the reviewers' comments, followed by our responses in blue, and a marked-up version of a revised manuscript with changes highlighted in yellow.

Reviewer Comments:

Reviewer #1

This article reports a wirelessly operated LED system that can optogenetically activate and inhibit neural activities, when combined with opsins like ReaChR and stGtACR2 as well as blue/green upconversion nanoparticles (UCPs). The red and IR LEDs are mounted on the surface of scalp without implantation, which minimizes the brain tissue damage. Wireless, bimodal neural modulations are successfully demonstrated in a mouse model, in multiple brain regions like M2, SC, mPFC, dmST. The paper is well written and has comprehensive animal studies. However, there are multiple issues that are needed to be addressed before the publication.

We much appreciate the reviewer's favorable consideration of our work and critical comments. We have attempted to address the reviewer's concerns by adding additional data and concrete explanations better to understand our work to reviewers and potential readers.

Major comments:

1. Thermal Issue: How hot is the LED? These LEDs are operated at a very high power (2.1 V, 0.25 A)? What is the temperature rise during the operation? How will it affect the mouse scalp and brain tissue? Some thermal measurements and simulations should be provided.

We greatly appreciate the reviewer's valuable comments. As the reviewer rightly pointed out, the LED requires high power, which can result in a continuous rise in temperature when operated without interruption. To prevent this, we used a 10% duty cycle for the LED and placed a small piece of plastic-based thermal isolator between the LED and the skull.

To verify the effectiveness of this approach, we conducted thermal measurements under several conditions: continuous LED operation, operation with a 10% duty cycle, and with or without the thermal isolator, as used in the experimental setup. Surface temperatures were recorded using a small PTC thermistor (NB-PTCO-001, Measurement Specialities) attached to the LED.

Our results revealed a rapid temperature increase during continuous operation, with peak temperatures reaching 77.9°C for the Red LED and 88.1°C for NIR LED due to overheating. However, when operated with a 10% duty cycle, the LEDs stabilized at 37°C (Red LED) and 39.1°C (NIR LED) due to the cooling period.

We further measured the temperature with the thermal isolator attached. When the LED with the thermal isolator was operated under the 10% duty cycle for 10 minutes, maximum temperatures of 34.5°C (Red LED) and 36.8°C (NIR LED) were measured. In this condition, temperatures remained below the body temperature of 37°C, indicating that heat from the LED is unlikely to cause brain damage. The results were further supported by our behavioral experiments.

However, without the thermal isolator, the NIR LED with a 10% duty cycle exceeded 39°C, which could potentially cause brain damage. A basic heat transfer calculation suggests that prolonged exposure could raise brain temperature beyond 39°C, highlighting the importance of the thermal isolator to safely operate the NIR LED without any potential damage.

Heat transfer equation

- Thermal conductivity of skull: 0.32 W/m·K [Žák, J. et al., *Mechatronics*, 2015]
- Skull thickness: 0.25 mm [Ghanbari, L. et al., *Sci Rep*, 2019]
- LED temperature: 39.1 °C

The temperature difference (ΔT) across the skull can be calculated using:

$$\mathrm{d}$$

$$\Delta T = k \times (T_{LED} - T_{brain})$$

Solving for the surface temperature on the brain:

$$0.00025 \quad 39.06945$$

$$T_{brain} = T_{LED} - \Delta T = 39.1 - (39.1 - T_{brain}) \times \_\_\_ \; 0.32 = \_\_\_ \; 1.0008 \approx 39.04 \; ^{\circ}C$$

The surface temperature of the brain would be slightly lower than the LED temperature of 39.1°C. Therefore, the thin mouse skull does not contribute to temperature reduction, and operating at a 10% duty cycle without the thermal isolator could result in severe brain damage [Owen et al., *Nat Neurosci*, 2019].

References:

1) Žák, J. et al. Model-based design of artificial zero power cochlear implant. *Mechatronics* 31, 3041, doi:10.1016/j.mechatronics.2015.04.018 (2015).
2) Ghanbari, L. et al. Craniobot: A computer numerical controlled robot for cranial microsurgeries. *Sci Rep* **9**, 1023, doi:10.1038/s41598-018-37073-w (2019).
3) Owen, S. F., Liu, M. H. & Kreitzer, A. C. Thermal constraints on in vivo optogenetic manipulations. *Nat Neurosci* **22**, 1061-1065, doi:10.1038/s41593-019-0422-3 (2019).

In conclusion, our experimental results showed that, under the given condition (LED with the thermal isolator, 10% duty cycle), tissue damage caused by heat from the LED was negligible. We have included these results, including the corresponding figures, in the Results and Methods sections of the manuscript to provide detailed information.

We have added the following statements related to thermal issues in the revised Results [lines 158-178 on pages 6-7] and Methods [lines 530-542 on page 17].

Results

Thermal effects of LED operation

To evaluate the potential for tissue damage by heat from LED operation, we measured the surface temperature of the LEDs and estimated the corresponding temperature increase in the brain tissue (Supplementary Table 2 and Supplementary Fig. 6). During continuous operation, the LED temperature rapidly increased, reaching a maximum of 77.9°C for the Red LED and 88.1°C for the NIR LED due to overheating (Supplementary Fig. 6b). However, when operated with a 10% duty cycle, the LEDs maintained stable temperatures of 37°C for the Red LED and 39.1°C for the NIR LED, aided by adequate cooling (Supplementary Fig. 6c). In addition, we attached a plastic-based thermal isolator to limit light dispersion and measured the temperature at the end. Under the 10% duty cycle with the thermal isolator attached, during 10 minutes of operation, the maximum temperatures were 34.5°C for the Red LED and 36.8°C for the NIR LED (Supplementary Fig. 6d). These temperatures are below body temperature (37°C), indicating that the heat from the LED is unlikely to cause brain damage.

However, operating the NIR LED at 10% duty cycle without the thermal isolator resulted in

temperatures exceeding 39°C, which could potentially cause brain damage[28]. Using Fourier's Law of heat conduction, we calculated the temperature change across the skull and found that the heat transferred to the brain could exceed 39°C, indicating a risk of brain damage with prolonged exposure (Supplementary Note 1).

These results suggest that under specific conditions (LED with thermal isolator, 10% duty cycle), the potential for thermal stimulation or cell damage due to LED operation is low.

Methods

Thermal measurements of LED operation

To address the potential thermal issues associated with the high-power operation of LEDs, we employed a 10% duty cycle to prevent continuous temperature increases. Thermal measurements were performed under various conditions, including constant LED operation, 10% duty cycle operation, and with and without the attachment of a plastic-based thermal isolator of thermal isolator used in the experimental setup.

A small PTC thermistor (NB-PTCO-001, Measurement Specialties) was attached to the measurement pad to monitor surface temperature (Supplementary Fig. 6a). We continuously tracked the changing resistance of the thermistor in real time and calculated the temperature using the formula provided in the datasheet. This setup enabled us to capture the maximum temperature under conditions closely mimicking the experimental setup, ensuring accurate assessments of the potential impact on brain tissue. Maximum temperature was recorded after 10 minutes of LED operation under each condition.

Also, we have included an estimation of the surface temperature of the brain caused by heat from the LED in Added Supplementary Note 1.

Supplementary Note 1. Estimation of the surface temperature of the brain caused by heat from the LED

To estimate the surface temperature of the brain caused by heat from the LED, we measured the temperature of the LED during operation.

The temperature difference (ΔT) across the skull can be calculated using:

$$\Delta T = \frac{d}{k} \times (T_{LED} - T_{brain})$$

In the equation, ΔT is the temperature difference, d is the skull thickness, and k is the thermal conductivity of the skull.

For example, if the LED temperature is 39.1°, we can estimate the surface temperature above the equation.

- Thermal conductivity of skull[6]: 0.32 W/m·K
- Skull thickness[7]: 0.25 mm
- LED temperature: 39.1°C

$$T_{brain} = T_{LED} - \Delta T = 39.1 - (39.1 - T_{brain}) \times \frac{0.00025}{0.32} = \frac{39.06945}{1.0008} \approx 39.04°C$$

This LED temperature can cause severe damage to the brain[8].

Also, we have included the measurement data in the Added Supplementary Table.

Added Supplementary Table 2

	Resistance (Ω)	Temperature (°C)
Red, continuous operation, without the plastic-based thermal isolator	130.1	77.9
NIR, continuous operation, without the plastic-based thermal isolator	134.0	88.1
Red, 10 Hz, 10 ms (10% duty cycle), without the plastic-based thermal isolator	114.4	37.0
NIR, 10 Hz, 10 ms (10% duty cycle), without the plastic-based thermal isolator	115.2	39.1
Red, 10 Hz, 10 ms (10% duty cycle), with the plastic-based thermal isolator	113.4	34.5
NIR, 10 Hz, 10 ms (10% duty cycle), with the plastic-based thermal isolator	114.3	36.8

Supplementary Table 2: Thermal measurements of LED operation under various conditions. This table presents the resistance and corresponding temperature measurements for red and NIR LEDs under various operational conditions. The temperatures were calculated using the calculation formula provided by the provider.

$$(T) = R(0)\,x\,(1 + a\,x\,T + b\,x\,T\$)$$

where $R(T)$ is the resistance at temperature T,

(0) = 100Ω, which is the resistance at 0°C,

$a = 3.9083 x\ 10^{\%\&}$,

$b = -5.775 x\ 10^{\%(}$.

The temperature measurement includes an error margin of $\pm\ *0.15 + 0.002\,x\ +,^{\circ}\text{-}\overline{+}.°C$, reflecting the precision of the thermistor.

Also, we have included the results for thermal measurements in the Added Supplementary Figure.

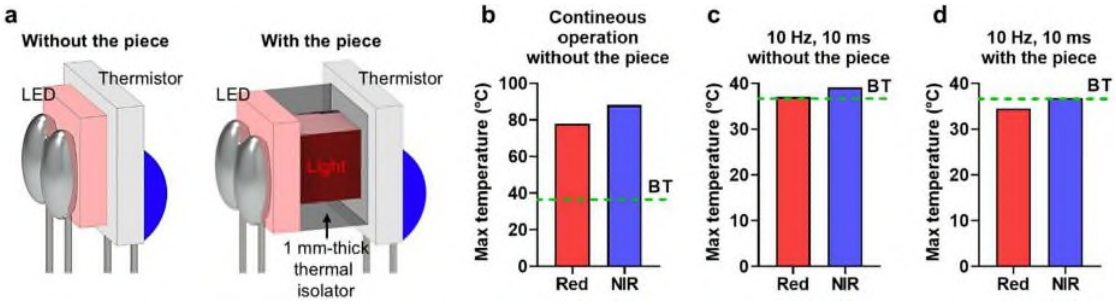

Supplementary Fig. 6: Thermal measurements of Red and NIR LEDs with and without a plastic-based thermal isolator. a Schematic of the thermal measurement setup. Illustrations showing the experimental setup used for measuring the temperature of LEDs, both with and without a 1 mm-thick

thermal isolator of thermal isolator. A thermistor is attached to record temperature changes during LED operation. **b** Maximum temperature during continuous operation without the thermal isolator. **c** Maximum temperature at 10 Hz, 10 ms without the thermal isolator. **d** Maximum temperature at 10 Hz, 10 ms with the thermal isolator. In each graph, the dotted line labeled "BT" indicates the body temperature of a mouse, which is 36.6°C.

2. Power Issue: How long can the battery last? The battery used in the circuit has a capacity of 30 mAh. The LED is operated at 2.1 V, 0.25 A, 50% duty cycle. Based on a simple estimation, the battery can only last for <15 mins if only one LED is on. To operate multiple LEDs, the battery lifetime will be even shorter.

We apologize for the lack of detailed information and sincerely thank the reviewer for pointing it out. In the electrophysiological experiments, the LED was operated at 2.1 V, 0.25 A with a 0.5 Hz frequency and 50% duty cycle. An external power supply for LED operation was used as the experiments were conducted on anesthetized mice. Additionally, a small heatsink (9 x 9 x 5 mm^3) was attached to the LED during the experiments to dissipate heat, and the LED was positioned 1-2 mm away from the skull due to the difficulty of attaching the LED directly to the skull with the probe implanted in the brain.

In all behavioral experiments, the operating condition of the LED was 2.1 V, 0.25 A, with a 10% duty cycle. We have added this previously missing information in the revised Results [lines 180-205 on page 7] and Methods [lines 626-637 on pages 19-20].

Results

Transcranial optogenetic modulation of neurons in vivo

The initial objective of our study was to evaluate the feasibility of our optogenetic strategy in animals by determining the efficacy of transcranial modulation and the stimulation depth, which is dependent on the combination of the virus, LED, and particles (e.g., stGtACR2–NIR–Blue UCP) in vivo. To achieve this goal, we conducted electrophysiology experiments using three combinations (ReaChR–Red LED, ReaChR–NIR LED–Green UCP, and stGtACR2–NIR LED–Blue UCP) (Supplementary Fig. 7) (The detailed experimental protocol, including surgery and experimental setup, is provided in the Methods section). After injecting viruses and particles into various brain regions (cortex, hippocampus, and thalamus) (Supplementary Fig. 7), we allowed four weeks for sufficient infection. We then inserted a neural probe with 16 black platinum microelectrodes into the infected regions of each mouse (Supplementary Fig. 7).

In the first experiment, we measured neural activation using red light on the skull of a mouse infected with the ReaChR virus. In the sensory cortex region, we successfully observed a statistically significant increase in neural signals with red light illumination at 63 $mW \cdot mm^{-2}$ (2.1 V, 0.25 A) with 0.5 Hz, 50% duty cycle (Supplementary Figs. 8a-c). However, no increase in neural activity was observed in the hippocampal CA3 region (Supplementary Figs. 8d-e). Our results confirm the feasibility of transcranial neural activation up to a depth of approximately 0.7 mm, including the skull thickness (approximately 0.2 mm), using the ReaChR virus and red LED.

Next, we measured neural activation using NIR light on the skull of a mouse infected with the ReaChR virus and injected with green UCPs. We observed a statistically significant increase in neural signals in the thalamus region when NIR light was applied at 275.5 $mW \cdot mm^{-2}$ (2.6 V, 0.25 A) with 0.5 Hz, 50% duty cycle (Supplementary Figs. 9a-c). Our results confirmed that transcranial neural activation was possible up to a depth of approximately 3 mm, accounting for skull thickness, using the ReaChR virus, NIR LED, and green UCPs.

Methods

Electrophysiological experiment and neural signal analysis

To evaluate transcranial neuromodulation in vivo under various combinations of viruses, LED, and particles, we used a silicon-based neural probe integrated with 16 black Pt microelectrodes (14 x 14 μm^2) to measure neural activity by light. The neural probe was prepared using a previously reported method[38], with 16 recording electrodes spaced 40 µm apart on a single shank. The probe had a width of 128 µm and a thickness of 20 µm. The average impedance of the electrodes was 17 ± 1 kΩ at 1 kHz. Additionally, the LED was operated at 2.1 V and 0.25 A with a 0.5 Hz, 50% duty cycle. An external power supply was used for LED operation for these experiments as the mice were anesthetized. A small heatsink (9 x 9 x 5 mm^3) was attached to the LED to dissipate heat, and the LED was positioned 1-2 mm away from the skull due to the difficulty of attaching the LED directly to the skull with the probe implanted in the brain.

We also assessed the system's operating time using a fully charged 30 mAh battery. The Red LED and NIR LED each operated for approximately 53 minutes. When both LEDs were operated simultaneously, the battery lasted approximately 26 minutes. As the reviewer noted, high-power LEDs result in a short operating time of around 1 hour, which is further reduced when multiple LEDs are used simultaneously.

For future research, we suggest that using a laser diode (LD) with higher directionality could improve efficiency. Laser diodes (LDs) offer several advantages over LEDs, including greater directionality and better power efficiency. At higher input power densities, LDs can reach power-conversion efficiencies of around 30% compared to just 5% of LEDs [Wierer Jr et al., *Laser & Photonics Reviews*, 2013]. This makes LDs particularly suitable for applications requiring focused, high-power efficiency light.

Furthermore, previous studies found minimal impact on mice activity levels with devices weighing up to 5 g [Shin et al., *Nature Comm*, 2022]. Since our current device weighs less than 2 g, increasing the battery capacity is feasible for long-term behavioral experiments. This suggests that enhancing battery capacity is both achievable and necessary for such studies. We have added these measurement results to the revised Results section [lines 133-139 on page 5] and discussed the current research limitations regarding operating time and potential solutions in the revised Discussion section [lines 434-449 on page 14].

References:

1) Wierer Jr, J. J. et al, Comparison between blue lasers and light-emitting diodes for future solid-state lighting. *Laser & Photonics Reviews*, **7(6)**, 963-993, (2013).
2) Yoon, Y. et al. Neural probe system for behavioral neuropharmacology by bi-directional wireless drug delivery and electrophysiology in socially interacting mice. *Nat. Commun.* **13**, 5521, doi:10.1038/s41467-022-33296-8 (2022).

Results

Additionally, we assessed the operating duration of the system using a fully charged 30 mAh battery. The red and NIR LEDs were operated for approximately 53 min each. However, when both the LEDs were operated simultaneously, the battery life decreased to approximately 26 min. Consequently, the high-power consumption of LEDs limited their operating time to approximately 1 h, which decreased further when multiple LEDs were used concurrently. An operating time of approximately 1 h is sufficient for conducting short-term behavioral experiments[25-27].

Discussion

In future work, incorporating laser diodes (LDs) with superior directionality can significantly enhance system performance. Unlike LEDs, LDs provide distinct advantages such as higher directionality and improved power efficiency. LDs with high directionality can provide superior spatial resolution and

enable the stimulation of deeper brain regions. Additionally, LDs can handle much higher power densities and maintain power conversion efficiencies of approximately 30%, making them ideal for experiments requiring concentrated and intense light[41]. Moreover, LDs do not experience an efficiency droop at higher power levels, which is a common issue with LEDs[41], making them more suitable for sustained high-power use. Therefore, integrating high-power LDs could extend the applicability of our approach from animal models such as mice to potential human applications.

Furthermore, our previous research indicated that mice exhibit minimal impact on activity levels with weights up to 5 g[26]. Given that our current device weighs < 2 g, there is substantial room to increase the battery capacity without adversely affecting the behavior of the mice. Enhancing battery capacity is both feasible and critical for the success of long-term behavioral studies, as it would allow for extended operational times, effectively meeting the demands of such experiments

3. Optical Issue: What are the spectral overlap of ReaChR, stGtACR2, red LED, NIR LED, blue and green UCPs? Excitation spectra of opsins (ReaChR and stGtACR2) and emission spectra of light sources (LEDs and UCPs) should be presented together, so we can check their overlaps. It is speculated that when ReaChR and stGtACR2 are co-expressed in the same region, green light would excite both of them.

We apologize for the lack of information regarding the spectral overlap and greatly appreciate the reviewer's valuable comment. In response, we have added the overlapping spectral graphs of the viruses, LEDs, and UCPs used in our study to the revised supplementary information.

Added Supplementary Figure 5

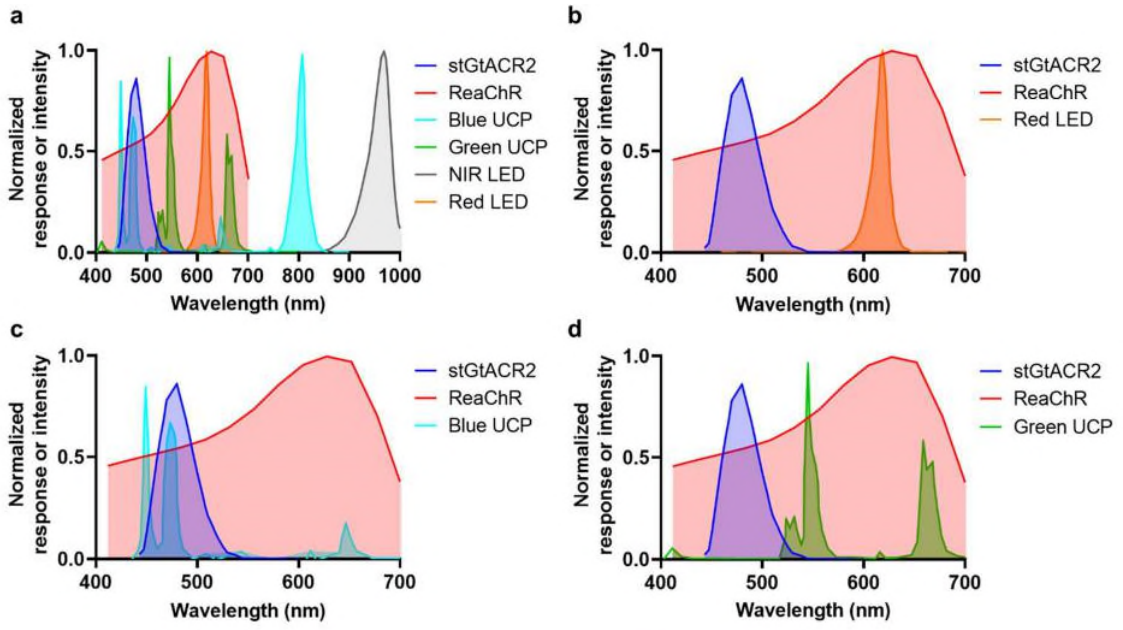

Supplementary Fig. 5: Spectral overlap of opsins and light sources. a Full spectral analysis. The normalized response or intensity spectra of stGtACR2, ReaChR, Blue UCP, Green UCP, NIR LED, and Red LED. **b** The spectral overlap between the Red LED, ReaChR, and stGtACR2. **c** The spectral overlap between the Blue UCP, ReaChR, and stGtACR2. **d** The spectral overlap between the Green UCP, ReaChR, and stGtACR2.

We analyzed the overlapping spectra and found that the green UCP has a narrow spectrum with a peak wavelength of 550 nm and local peak at 520 nm. At 520 nm, stGtACR2 shows a response efficiency of approximately 10%, while ReaChR exhibits around 70% efficiency at 550 nm. Based on

these findings, we anticipate that the green UCP can selectively activate ReaChR without triggering stGtACR2. In our experiment, we used a Red LED to activate ReaChR and blue UCP to activate stGtACR2 in mPFC. However, for the control of neural activity in deeper brain regions, we expect to use glue UCP and green UCP for the selective activation of ReaChR and stGtACR2, respectively

We have added these predictions and detailed analyses in the revised Results to comprehensively understand the spectral overlaps [lines 140-155 on page 5].

To further investigate the feasibility of bimodal neuromodulation using different combinations of viruses, UCPs, and LEDs, we analyzed the overlapping spectra of each component (Supplementary Fig. 5). Our analysis showed no overlap between the emission wavelength of the Red LED and the response wavelength of stGtACR2 (Supplementary Fig. 5b); however, there was a significant overlap with the response wavelength of ReaChR (Supplementary Fig. 5b). This indicates that neuronal activation via ReaChR using the Red LED is feasible. Additionally, the emission wavelength of the Blue UCP generated by the NIR-Blue UCP combination overlaps with the response and peak wavelengths of stGtACR2 (Supplementary Fig. 5c). However, the response of ReaChR to the NIR-Blue UCP combination was approximately 60% of that of stGtACR2, enabling selective neuronal inhibition through stGtACR2. Furthermore, the Green UCP exhibited a narrow emission spectrum with a peak at 550 nm, and the response efficiency of ReaChR was substantially higher than that of stGtACR2 (Supplementary Fig. 5d). Thus, to control neural activity in deep brain regions, we used blue and green UCPs to selectively activate ReaChR and stGtACR2, respectively. Overall, these results confirm that bimodal neuromodulation is feasible using various combinations based on the spectral overlap analysis.

4. Resolution Issue: What is the spatial resolution for external light stimulation? Optical modeling can be used to evaluate the volume of a brain region that is modulated when light is applied extracranially. The paper claims that its technique has "high spatial resolution", but it is doubtful. The light distribution will be widespread after passing through the skull. Therefore, its spatial resolution should be inferior to implantable light sources.

We greatly appreciate the reviewer's valuable comments and have performed simulations to access the spatial resolution of external light stimulation. Before running the Monte Carlo simulation, we measured the light dispersion angle of the red LED with the square piece (thermal isolator) attached to control the light spread. We conducted the measurements in a dark environment with the distance between the LED and a paper ruler from 1 mm to 4 mm.

The observed light spread ranged 2 mm, 3 mm, 4 mm, and 5 mm at respective distances of 1 mm, 2 mm, 3 mm, and 4 mm, respectively. Using the simple mathematical calculations below, we verified that the light dispersion angle in the air was 53.14°.

The divergence angle (a) was calculated using the tangent function:

$$\tan\left(\frac{a}{2}\right) = \frac{\Delta 7}{2\Delta 8}$$

In the equation, $\Delta 7$ is the change in the width of the light beam, $\Delta 8$ is the change in distance.

For example, from 1 mm to 2 mm

Width at 1mm (7_9): 2 mm

Width at 2mm (7_8): 3 mm

Distance Difference ($\Delta 8$): 2 mm – 1 mm = 1 mm

Width Difference ($\Delta 7$): 3 mm – 2 mm = 1 mm

Using the equation:

$$\tan\left(\frac{a}{2}\right) = \frac{\quad}{\quad}\frac{\quad}{1}$$

$$2 \times 1 = 21$$

$$\alpha = 2 \times \arctan(1/2) \approx 2 \times 26.57^\circ = 53.14^\circ$$

Using the measured light dispersion angle in the air and the optical properties of the mouse skull and tissue, we performed Monte Carlo simulations to access the light spread within the brain [Fang, Q. Q. et al., *Opt. Express*, 2009 and Fang, Q. Q. et al., *Opt. Express*, 2010]. The simulation results showed that about 10% of the light penetrated to a depth of 1.25 mm and extended laterally up to 0.75 mm at a depth of 1 mm. This suggests that the spatial resolution of the light, when using the Red LED to stimulate ReaChR-infected neurons directly, was predicted to be approximately 0.75 mm. Our behavioral experiments support this result, demonstrating selective stimulation of the left and right M2 regions.

While we acknowledge that the spatial resolution is inferior to implantable light sources, the resolution of our proposed approach is also affected by the volume of the injected particle. Through the c-fos analysis, we confirmed the spatial resolution of 0.5 mm in the striatum region. We also expect that the resolution could be further improved by carefully controlling the injection volume.

References:

1) Fang, Q. Q. & Boas, D. A. Monte Carlo simulation of photon migration in 3d turbid media accelerated by graphics processing units. *Opt. Express* **17**, 20178–20190 (2009).

2) Fang, Q. Q. Mesh-based Monte Carlo method using fast ray-tracing in Plucker coordinates. Biomed. *Opt. Express* **1**, 165–175 (2010).

We have added the following statements related to the resolution issue in the revised Results [lines 288-307 on page 10] and Methods [lines 681-694 on page 21].

Results

Simulations were also conducted to evaluate the spatial resolution achievable with external light stimulation using a red LED. Prior to the simulations, we measured the light dispersion angle of the red LED with the square thermal isolator attached to limit the light spread. These measurements were conducted in a dark environment, with distances ranging from 1 to 4 mm between the LED and a paper ruler (Supplementary Fig. 18a). We observed that the light spread ranged from 2, 3, 4, and 5 mm at distances of 1, 2, 3, and 4 mm, respectively (Supplementary Table 3). Using basic mathematical calculations, we determined that the light dispersion angle in air was approximately 53.14° (Supplementary Note. 2). Using this dispersion angle and the optical properties of the mouse skull and tissue for red light[17,35], we performed Monte Carlo simulations to evaluate light spread within the brain[36,37]. The simulations indicated that approximately 10% of the light reached a depth of 1.25 mm and extended laterally up to 0.75 mm at a depth of 1 mm (Supplementary Fig. 18b). Hence, the estimated spatial resolution of the light when targeting ReaChR-infected neurons was approximately 0.75 mm. To avoid overlap and crosstalk between the two light sources, a minimum separation of 1.5 mm would be necessary. In our behavioral experiments, we successfully achieved the expected effects by independently stimulating the left or right cortex (left M2 or right M2). This success was likely due to a larger population of neurons responding within the targeted region. Although the spatial resolution of our LED-based system has certain limitations, clear differences in the extent of stimulation and the number of responsive cells in adjacent areas allowed for successful selective behavioral modulation.

Methods

Simulation of light distribution within the brain

To estimate the light distribution from the red LED within the brain for optical stimulation, we utilized Monte Carlo simulations (Monte Carlo eXtreme; MCX)[36,37]. In the simulation, we modeled the skull and brain tissue using a domain size of 250 × 250 × 250 with 0.1 mm voxels.

For the skull (250 x 250 x 25 of domain size), we applied an absorption coefficient of 0.6 mm^{-1}, a scattering coefficient of 2.5 mm^{-1}, an anisotropy factor of 0.92, and a refractive index of 1.36[49]. For brain tissue (250 x 250 x 225 of domain size), we used an absorption coefficient of 0.4 mm^{-1}, a scattering coefficient of 4 mm^{-1}, an anisotropy factor of 0.92, and a refractive index of 1.36[50]. These parameters were chosen to accurately represent the optical properties of both the skull and brain tissues under red light illumination.

The light source was positioned at voxel (125, 125, 0) with a dispersion angle of 53.14°. A total of 1.96×10^{17} photons·ms^{-1} were emitted from the light source, reflecting the optical power of the red LED. This setup allowed us to evaluate the light intensity and spread across the cortical regions.

Also, we have included a calculation of the divergence angles for the light spread from the LED in Added Supplementary Note 2.

Supplementary Note 2. Calculation of the divergence angles for the light spread from the LED

To calculate the angle of divergence of the LED light source used in our experimental setup, we measured the light spread by placing a paper ruler at distances ranging from 1 mm to 4 mm from the LED. This setup allowed us to measure the diameter of the range of divergence at each distance.

The angle of divergence (1) was calculated using the tangent function:

$$\tan 5^{1}{}_{2}6 = \frac{\Delta 7}{2\Delta 8}$$

In the equation, $\Delta 7$ is the change in the width of the light beam, $\Delta 8$ is the change in distance.

For example, from 1 mm to 2 mm

- Width at 1mm (7_{9}): 2 mm
- Width at 2mm ($7_{\$}$): 3 mm
- Distance Difference ($\Delta 8$): 2 mm – 1 mm = 1 mm
- Width Difference ($\Delta 7$): 3 mm – 2 mm = 1 mm

Using the equation:

$$\tan 5^{1}{}_{2}6 = \frac{1}{2 \times 1 = 2}1$$

$$1 = 2 \times \arctan :^{1}{}_{2}; \approx 2 \times 26.57° = 53.14°$$

Also, we have included light dispersion and simulation of LED operation in Added Supplementary Figure 18.

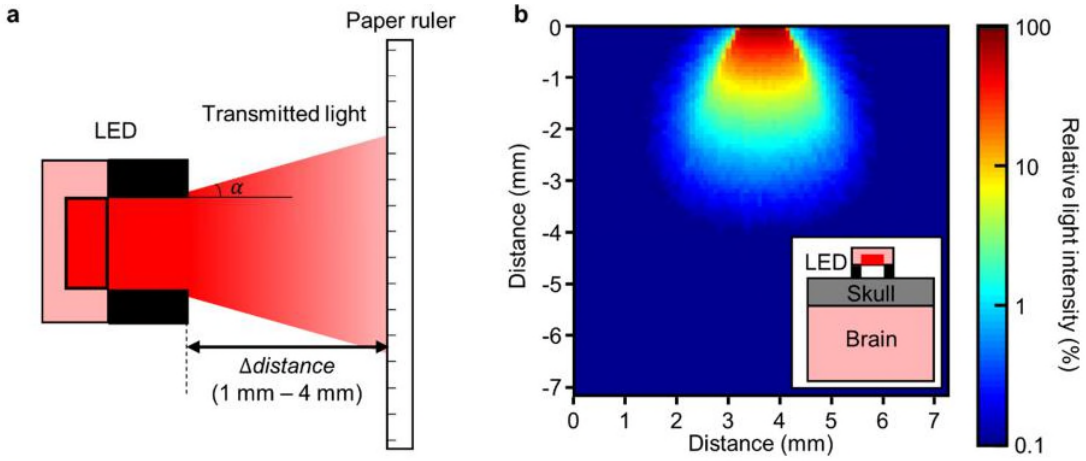

Supplementary Fig. 18: Light dispersion and simulation of LED operation. a Schematic representation of light dispersion measurement. The experimental setup used to measure the light dispersion angle (1) of the red LED. A paper ruler is positioned at varying distances (1 mm to 4 mm) from the LED to quantify the spread of transmitted light. The square piece is attached to the LED to limit the light spread. **b** Simulated light distribution within brain tissue. The Monte Carlo simulation results show the relative light intensity distribution within the brain, modeled to reflect in vivo conditions. The inset illustrates the position of the LED, skull, and brain.

5. Viral Expression Issue. In the fluorescence images (Fig. 2b, S11, S12), the viral expressions are not clear at all, and cell bodies cannot be distinguished. It is difficult to tell if the opsin expressions (ReaChR and stGtACR2) are successful. For example, in Fig. 2b, it is impossible to count how many cells are expressed with ReaChR under different injection doses. Also, DAPI staining is suggested to use to label the cell body.

We greatly appreciate the reviewer's valuable comments and suggestions. We initially captured low-magnification images to visualize the overall range of viral expression. However, at this magnification, we found that cell bodies and neurites were not clearly distinguishable, a limitation also note in previous studies [Tinterri, A. et al., *Nat Commun*, 2018 and Chou, N. et al., *Adv Sci*, 2022].

References:

1) Chou, N. et al. A Multimodal Multi-Shank Fluorescence Neural Probe for Cell-Type-Specific Electrophysiology in Multiple Regions across a Neural Circuit. Adv Sci (Weinh) 9, e2103564, doi:10.1002/advs.202103564 (2022).

2) Tinterri, A. et al. Active intermixing of indirect and direct neurons builds the striatal mosaic. Nat Commun 9, 4725, doi:10.1038/s41467-018-07171-4 (2018).

To address this issue, we performed additional high-magnification imaging to confirm neuronal cell staining. At higher magnification, we were able to clearly observe the morphology of the neuronal cells including neurites. Following the reviewer's recommendation, we also included DAPI-stained images to label the cell bodies.

These high-magnification and DAPI-stained images provide a more detailed visualization of opsin expression in infected neurons, allowing for more detailed visualization of opsin expression in infected neurons, enabling a more accurate assessment of the number of cells expressing ReaChR-expressing cells at different injection doses. We have included these images and supplementary information in the revised manuscript.

Revised Figure 2

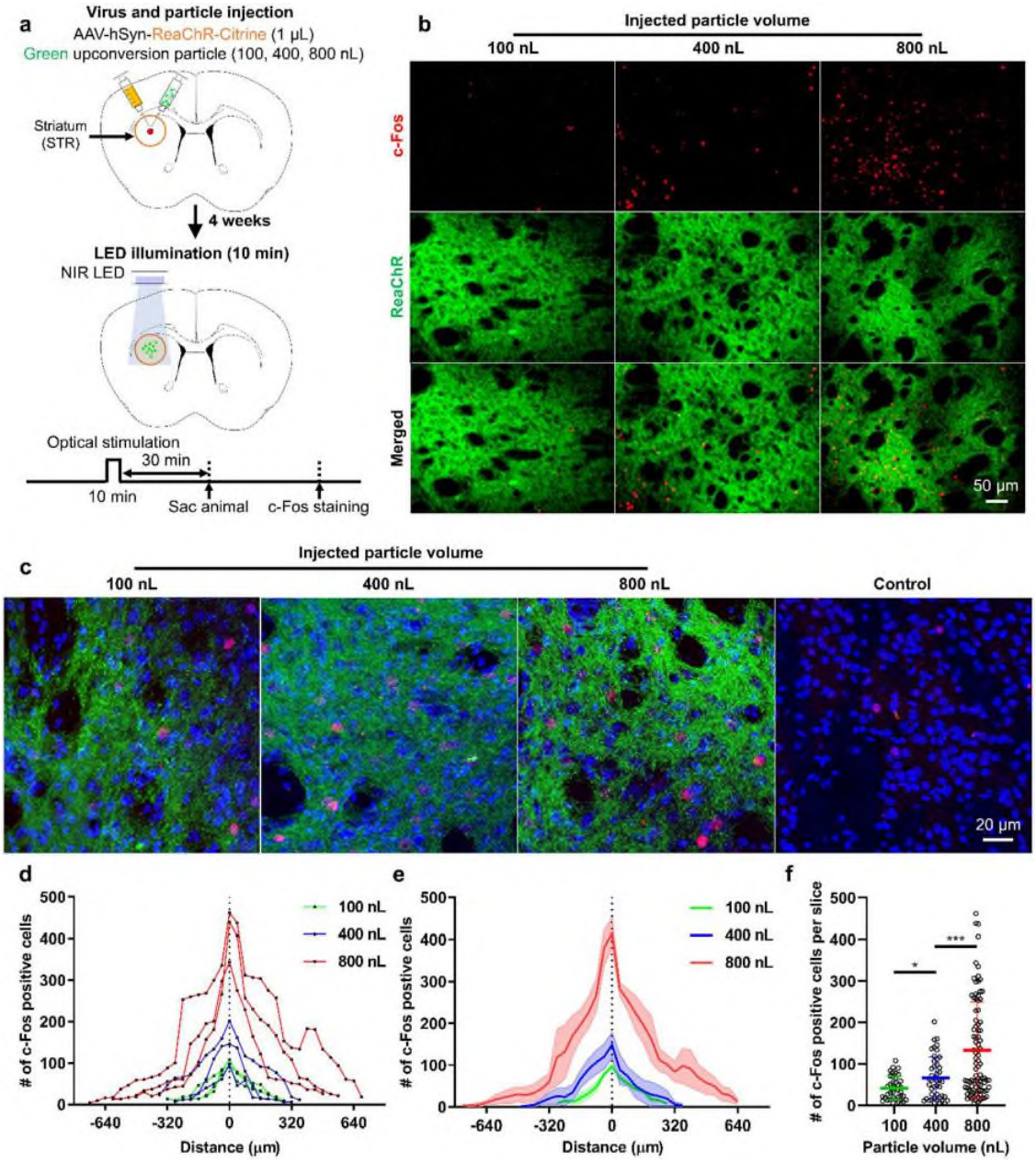

Fig. 2: Spatial resolution of transcranial brain optogenetic method in vivo. a Schematic diagrams of virus/particle injection and experimental process. ReaChR virus was injected into striatum (STR). Green upconversion particles of varying quantities (100, 400, and 800 nL at a concentration of 20 $mg \cdot mL^{-1}$) were injected into the same region. After 4 weeks, the c-Fos expression experiment was conducted. **b** The expression of c-Fos in the target region according to the quantities of the particles. **c** High magnification image of c-Fos expression. The control group consists of mice that underwent NIR stimulation without any injection of virus or particles. In the image, red represents c-Fos expression, green indicates ReaChR virus-infected neurons, and blue represents DAPI (labeling cell nuclei). **d** The number of c-Fos positive cells according to the volume of particles injected into individual mice. Three mice were used for each condition. Each data point represents the number of c-Fos positive cells in a 40-μm brain slice. **e** The number of c-Fos positive cells according to the volume of particles. The bold colored lines represent the mean value from the three mice. The lighter shade represents the standard

error of the mean (SEM). **f** The number of c-Fos positive cells per slice according to the volume of particles (100 nL-400 nL: t(82)=2.616, p=0.1057445, 400 nL-800 nL: t(134)=3.708, p=0.00030456; n=39 for 100 nL; n=45 for 400 nL; n=91 for 800 nL where n is the number of slices exhibiting c-Fos expression from three mice.). Statistical analysis was performed by the two-tailed unpaired t test, and p<0.05 was considered significant. * p< 0.05, *** p< 0.001.

Added Supplementary Figure 11

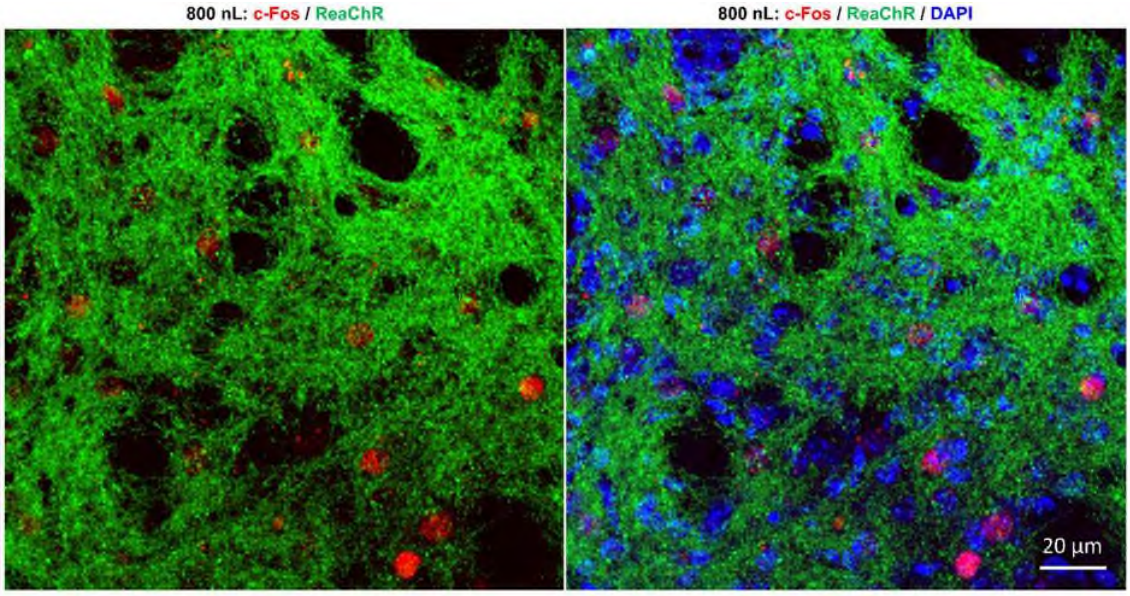

Supplementary Fig. 11: High-magnification representative confocal fluorescence images showing c-Fos expression induced by NIR stimulation in mice injected with virus and particles (800 nl). (Left) Image showing virus-infected neurons and c-Fos expression. (Right) Image showing virus-infected neurons, c-Fos expression, and DAPI staining.

Added Supplementary Figure 12

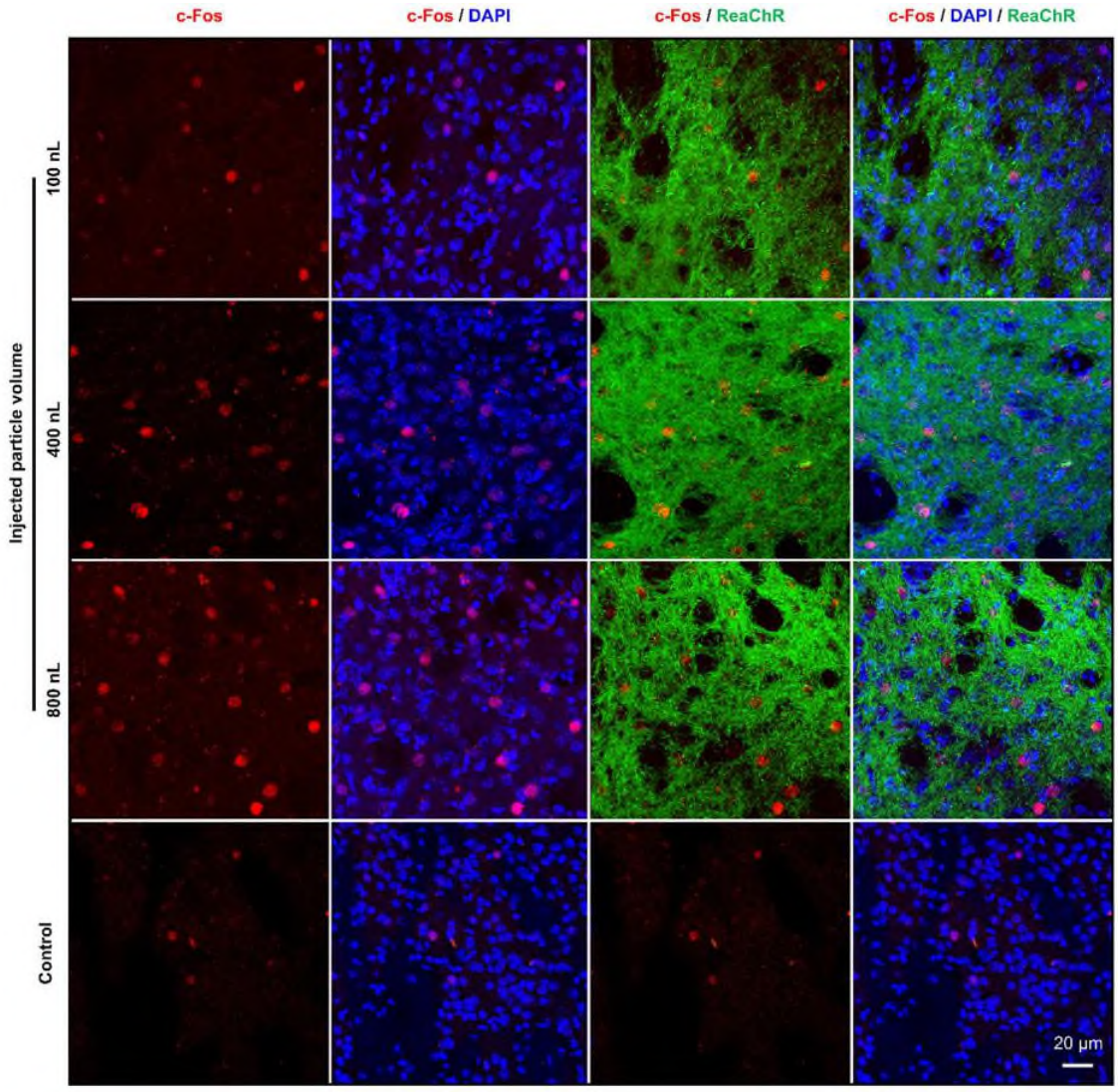

Supplementary Fig. 12: High-magnification fluorescence images showing c-Fos expression in the target region depending on the amount of particle injection. The control group represents mice that underwent NIR stimulation without the injection of both virus and particles.

Other minor issues:

6. Fig. S1, please label the intracellular and extracellular regions, and double check the ion flow direction for ReaChR. Should K+ ions flow in or out?

We appreciate the reviewer's insightful comments and apologize for any confusion. As the reviewer correctly pointed out, for ReaChR, only Na+ and Ca2+ ions flow into the membrane, while K+ ions do not. We have revised Figure S1 by removing the K+ ions and labeling the ions according to their respective colors.

Revised Supplementary Fig 1

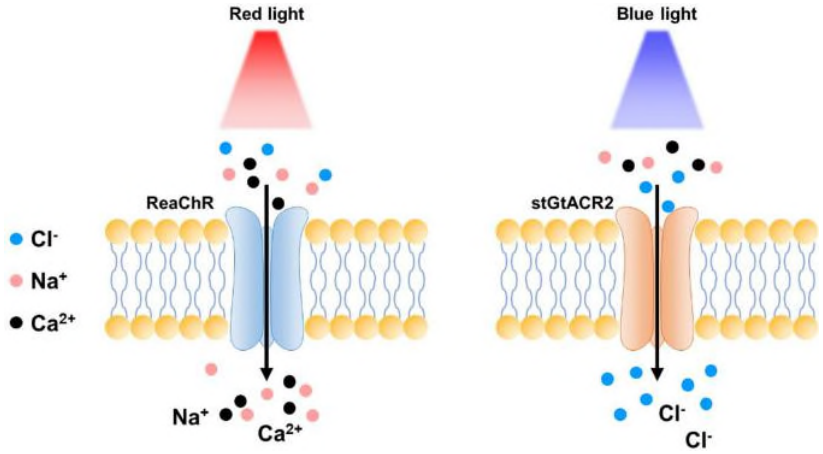

Supplementary Fig. 1: Schematic diagram of optogenetic modulation at the cellular scale. The process involves using light to regulate the activity of specific channels in cells. In this case, the cation channel ReaChR is depolarized by red light, while the anion channel stGtACR2 is hyperpolarized by blue light.

7. Table S1, it is not fair to make such a comparison. For those invasive methods, their advantages are that they can reach very deep tissue. Therefore, it is suggested that at least the stimulation depth should be added in this table.

We appreciate the reviewer's valuable suggestion. As pointed out, invasive methods offer the advantage of accessing much deeper brain tissue compared to the method proposed in our study. In response, we have updated Table S1 to include the stimulation depth for a more accurate comparison.

	Proposed system	**[1]Li et al., 2022**	**[2]Kim et al., 2021**	**[3]Yang et al., 2021**
Invasive or non-invasive	**Non-invasive**	Invasive	Invasive	Invasive
Depth of stimulation	**~ 3 mm**	No limits	No limits	No limits
Multiple site modulation	**Yes**	No	Yes	Yes
Number of the sites	**4**	1	2	2
Bimodal modulation	**Yes**	Yes	No	No
LED's colors	**Red / NIR**	Blue / Red	Blue	Blue
Size (mm^2)	**19 x 12 mm^2**	22 x 13 mm^2	19 x 12 mm^2	10 x 12 mm_2

Weight (g)	**1.9 g (including 30 mAh LiPo battery)**	1.9 g (including 35 mAh Li-ion battery)	1.4 g (including 12 mAh LiPo battery)	< 1 g (wireless power transfer)

Supplementary Table 1: A summary of our device`s performance and comparison with previously developed wireless optoelectronic brain modulator.

8. Fig. 3: "p>0.999999999999999" is not a proper usage.

We appreciate the reviewer's valuable suggestion. As recommended, we have revised the p-value to four decimal places.

The updated p-value is now reflected in Figure 3 in the revised manuscript.

9. Fig, 4: "p<0.000000000000001" is not a proper usage.

We appreciate the reviewer's valuable suggestion. As advised, we have appropriately revised the p-value to four decimal places.

The updated p-value is now reflected in Figure 4 of the revised manuscript.

0. Line 141, "at 63 mW mm-2 (2.1 V, 0.25 A)". How and where to get the power density of 63 mW mm^{-2}?

We appreciate the reviewer's valuable suggestion and apologize for the lack of explanation. The optical power was measured using an optical power meter by coupling the LED with a photodetector and applying 2.1 V and 0.25 A. The optical power density was then calculated by dividing the measured optical power by the active region of the LED (1 mm x 1 mm).

We have added this explanation to the revised Methods for clarity [lines 522-528 on pages 16-17].

Optical power measurement

We used a photodetector (918D, Newport Inc., Irvine, CA, USA) in combination with an optical power meter (1936-R, Newport Inc., Irvine, CA, USA) to characterize the light output power from the LEDs. The end of the LED, coupled with the square piece (i.e., thermal isolator), was positioned near the photodetector to ensure accurate light intensity measurements. The fluctuation in output power was measured to be within ±0.002 mW, indicating stable light emission from the LED.

0. Line 48, "However, light must be delivered into the target region using an implanted fiber", not correct. Light can also be delivered using LED or waveguide based implants.

We appreciate the reviewer's correction. As pointed out, light can also be delivered through LED or waveguide-based implants. We have revised the sentence in the revised introduction accordingly [lines 48-50 on page 3].

Once the opsins are expressed, light must be delivered to the target region using an implanted fiber, light-emitting diode (LED), or waveguide-based implant to excite or inhibit opsin-tagged neurons.

Again, we appreciate the reviewer's valuable comments and believe our manuscript has improved significantly.

Reviewer Comments:

Reviewer #2

The manuscript 'Non-invasive wireless brain modulator for precise bimodal neuromodulation in multiple brain regions' by Shin et al. report their platform consisting of two-colored LEDs which can be wirelessly driven which can be used as a light source for optogenetics. The genetically modified channelrhodopsins ReaChR and soma targeted GtACR2 are tagged with upconverting nanoparticles (UCNPs) thus the exciting wavelengths are in the red an NIR spectral range. In vivo neuromodulation is performed leading to motion and behavioural control of mice.
I rate the importance of the published work in this subject area as top 30%. Novelty is in the top 50% as well. The scholarly representation needs further work in terms of English language, clarity and specificity of paragraphs. Especially the language should be checked by a native speaker. The methods are mostly testing the hypothesis, but not sufficiently described, both can be improved. I have some major concerns that have to be addressed and further evidence provided before considering this manuscript for publication.

We sincerely appreciate the reviewer's detailed feedback and valuable suggestions. Based on the reviewer's comments, we have made significant efforts to address the shortcomings and improve the manuscript. We have thoroughly revised the manuscript for clarity, specificity, and overall quality of the English language. A native English speaker has reviewed the revised manuscript for language accuracy.

Furthermore, we have expanded and clarified the Methods section to ensure a thorough description and comprehensive testing of the hypothesis. Specific details and explanations have been added to address the reviewer's important concerns and to provide the necessary evidence for consideration.

Again, we appreciate the reviewer's valuable comments and believe our manuscript has improved significantly.

Here are my detailed comments on the manuscript:

1. The authors claim that their technique is non-invasive, however, the genetic modification needs a craniotomy in order to insert the respective ChRs and UCNPs. Thus, it is arguable that the entire technique including the genetic modification is non-invasive. In the process the modulation is performed via transcranial light exposure, which is non-invasive, but only one part of the presented technique. Thus, the wording has to be changed accordingly to not misguide the readers.

We appreciate the reviewer's valuable suggestion. As pointed out, the term "non-invasive" could be misleading since the genetic modification requires a craniotomy. We have revised the manuscript to more accurately reflect the distinction, replacing 'non-invasive' with 'transcranial' to describe light exposure while acknowledging the invasive nature of the genetic modification process.

We have made the necessary changes in the title, abstract, introduction, and other relevant sections to prevent any potential misunderstandings.

Furthermore, we have provided a more detailed description of the transcranial optogenetic stimulation procedure to clarify any potential misunderstandings. This additional information has been included in the revised Introduction [lines 46-59 on page 3].

These opsins are typically delivered to target neurons via viral vectors, which necessitates a craniotomy to enable the virus to infect specific brain regions. Once the opsins are expressed, light must be delivered to the target region using an implanted fiber, light-emitting diode (LED), or waveguide-based implant to excite or inhibit opsin-tagged neurons.

Highly sensitive opsins and upconversion particles (UCPs) have recently been introduced for transcranial optogenetics. The opsins allow transcranial neuromodulation of the mouse brain, despite

the scattering and absorption of visible light in the brain tissue[7-10]. UCPs emit visible light by near-infrared (NIR) excitation with low scattering and absorption of light in tissues[11,12]. Although viral and UCP injections via craniotomy are similar to traditional optogenetic techniques, the key difference in transcranial optogenetic neuromodulation is that subsequent light delivery is performed extracranially. Following the initial viral and UCP injections, neural activity can be continuously modulated using only external light sources, eliminating the need for invasive implants.

2. In the list of NIBS mentioned, tNIRS should be named as well as this is best comparable to the presented work. Reference 10 is a good example for this.

We appreciate the reviewer's insightful suggestion. As recommended, we have included tNIRS (transcranial near-infrared stimulation) in the list of transcranial brain stimulation (TBI) techniques mentioned in the manuscript. tNIRS has been shown to have the potential as a non-invasive treatment for brain disorders. However, it is important to note that this stimulates all neural cells within the illuminated area, resulting in lower spatial resolution and a lack of cell-type-specific targeting.

We have added this information to the introduction of the revised manuscript [lines 38-43 on page 3], along with a discussion of its limitations compared to the technique presented in our work [lines 422-424 on pages 13-14].

Introduction

Specifically, prominent noninvasive brain stimulation technologies, such as transcranial magnetic stimulation (TMS), transcranial direct current stimulation (tDCS), and transcranial near-infrared stimulation (tNIRS), have been widely used as clinical tools for treating brain diseases[4-6]. However, most TBS techniques suffer from poor spatial resolution due to the spread of stimulation signals and nonspecific stimulation across different cell types, which makes precise neuromodulation difficult and may result in side effects[1].

Results

In particular, compared with tNIRS[6], our approach allows for localized, cell-type-specific stimulation within the regions in which the virus and UCPs have been injected.

Added reference:

Nizamutdinov, D., Ezeudu, C., Wu, E., Huang, J. H. & Yi, S. S. Transcranial near-infrared light in treatment of neurodegenerative diseases. Front Pharmacol 13, 965788, doi:10.3389/fphar.2022.965788 (2022).

1. In l.63 fiber and micro-LEDs are mentioned as invasive devices. For completeness micro-OLEDs should be added: https://www.nature.com/articles/s41928-023-01013-y

We appreciate the reviewer's valuable suggestion. As recommended, we have added micro-OLEDs to the list of invasive devices mentioned. The relevant sentence has been revised to include micro-OLEDs, and appropriate reference has been cited in the revised Introduction [lines 66-68 on page 3].

To achieve accurate and diverse modulation of neural circuits, invasive devices (e.g., fibers, micro-LED probes, and OLED probes, referring to organic light-emitting diode probes) have been developed for multi-site[15-19] or bimodal optogenetic neuromodulation[20].

Added reference:

Taal, A. J. et al. Optogenetic stimulation probes with single-neuron resolution based on organic LEDs

monolithically integrated on CMOS. Nature Electronics 6, 669-679, doi:10.1038/s41928-023-01013-y (2023).

3. In the abstract the authors very repeatedly and excessively use the terms (non-) invasive, and bimodal neurostimulation without giving much insight into the technique. Especially in the abstract the key findings are missing and should be described more precisely.

We appreciate the reviewer's valuable feedback. Based on the suggestion, we have revised the abstract to reduce the repetitive use of "transcranial" and "bimodal neuromodulation." Instead, we have used "transcranial optogenetic modulation" to more accurately describe the technique. Additionally, we have added the key findings to the abstract to provide clearer insights into our work. The revised abstract is as follows.

Abstract

Transcranial brain stimulation is a promising technology for safe modulation of brain function without invasive procedures. Recent advances in transcranial optogenetic techniques with external light sources, using upconversion particles and highly sensitive opsins, have shown promise for precise neuromodulation with improved spatial resolution in deeper brain regions. However, these methods have not yet been used to selectively excite or inhibit specific neural populations in multiple brain regions. In this study, we created a wireless transcranial optogenetic brain modulator that combines highly sensitive opsins and upconversion particles and allows for precise bimodal neuromodulation of multiple brain regions without optical crosstalk. We demonstrate the feasibility of our approach in freely behaving mice. Furthermore, we demonstrate its usefulness in studies of complex behaviors and brain dysfunction by controlling extorting behavior in mice in food competition tests and alleviating the symptoms of Parkinson's disease. Our approach has potential applications in the study of neural circuits and development of treatments for various brain disorders.

4. The characterization of the LEDs is entirely missing. There are no spectra shown, no jVP curves. Same holds for the UCNPs absorption. How does the spectral overlap look like, are the red and NIR emission spectra of the LEDs clearly separated? Is there a chance of crosstalk of the modulations? How does the overlap with ReaChR look like? There is only very poor information given on this, mainly just the power and power density, which is insufficient.

We apologize for the lack of information regarding the characterization of LEDs and the spectral overlap. Also, we greatly appreciate the reviewer's valuable comment. In response, we have added comprehensive characterization data for the LEDs and UCNPs, including comparisons of spectral overlap. The results show that the red and NIR emission spectra of the LEDs are clearly separated.

Additionally, we have included the overlapping spectral graphs of the viruses, LEDs, and UCPs used in our study in the revised supplementary information.

Added Supplementary Figure 5

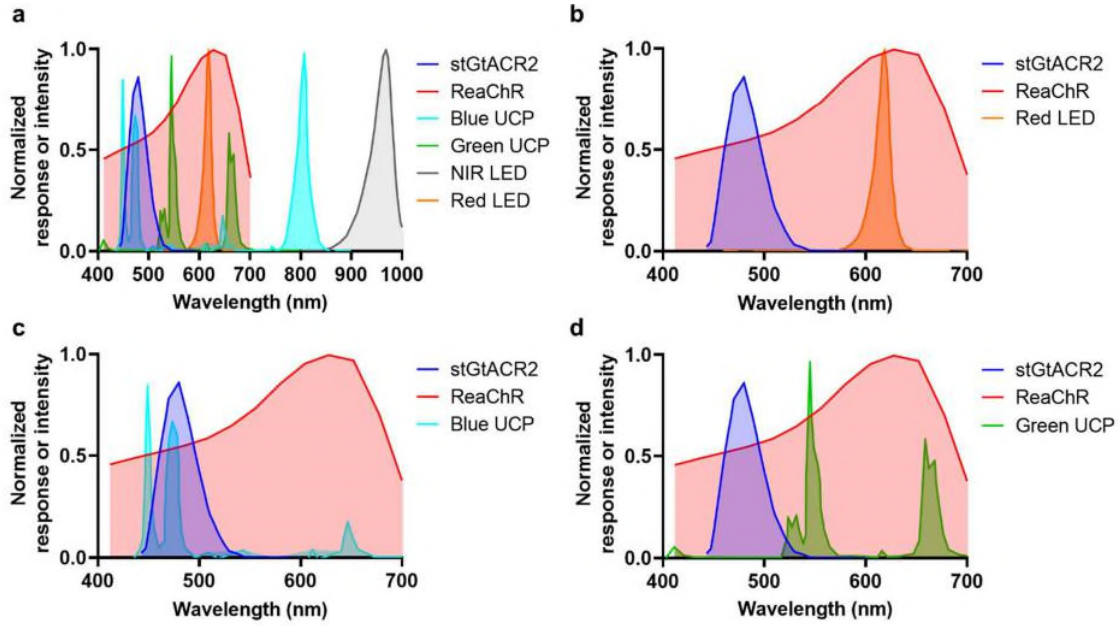

Supplementary Fig. 5: Spectral overlap of opsins and light sources. a Full spectral analysis. The normalized response or intensity spectra of stGtACR2, ReaChR, Blue UCP, Green UCP, NIR LED, and Red LED. **b** The spectral overlap between the Red LED, ReaChR, and stGtACR2. **c** The spectral overlap between the Blue UCP, ReaChR, and stGtACR2. **d** The spectral overlap between the Green UCP, ReaChR, and stGtACR2.

Upon analyzing the emission spectra of the red and NIR LEDs, we found that they are separated, minimizing the risk of crosstalk between the two light sources. The red LED emits at a wavelength that predominantly activates ReaChR, ensuring targeted neuromodulation with minimal interference from other spectral components. Moreover, the Blue UCP from the NIR-Blue UCP combination strongly overlaps the activation and peak wavelengths of stGtACR2, enabling efficient neuronal inhibition. In contrast, its overlap with the ReaChR activation range is approximately 60%, indicating reduced effectiveness in activating ReaChR. We have included these predictions and detailed analyses in the revised Results [lines 140-155 on page 6].

To further investigate the feasibility of bimodal neuromodulation using different combinations of viruses, UCPs, and LEDs, we analyzed the overlapping spectra of each component (Supplementary Fig. 5). Our analysis showed no overlap between the emission wavelength of the Red LED and the response wavelength of stGtACR2 (Supplementary Fig. 5b); however, there was a significant overlap with the response wavelength of ReaChR (Supplementary Fig. 5b). This indicates that neuronal activation via ReaChR using the Red LED is feasible. Additionally, the emission wavelength of the Blue UCP generated by the NIR-Blue UCP combination overlaps with the response and peak wavelengths of stGtACR2 (Supplementary Fig. 5c). However, the response of ReaChR to the NIR-Blue UCP combination was approximately 60% of that of stGtACR2, enabling selective neuronal inhibition through stGtACR2. Furthermore, the Green UCP exhibited a narrow emission spectrum with a peak at 550 nm, and the response efficiency of ReaChR was substantially higher than that of stGtACR2 (Supplementary Fig. 5d). Thus, to control neural activity in deep brain regions, we used blue and green UCPs to selectively activate ReaChR and stGtACR2, respectively. Overall, these results confirm that bimodal neuromodulation is feasible using various combinations based on the spectral overlap analysis.

Secondly, we measured the divergence angle of the LED with the square piece (i.e., thermal isolator) attached and included the results from the Monte Carlo simulation. Attaching the piece reduced the heat transmitted to the brain and decreased the divergence of the angle, thereby improving spatial resolution. The simulation results allowed us to predict the spatial resolution of light in studies utilizing integrated LEDs. We have added this information related to LEDs to the revised Results [lines 288307 on page 10] and Methods [lines 681-694 on page 21].

Results

Simulations were also conducted to evaluate the spatial resolution achievable with external light stimulation using a red LED. Prior to the simulations, we measured the light dispersion angle of the red LED with the square thermal isolator attached to limit the light spread. These measurements were conducted in a dark environment, with distances ranging from 1 to 4 mm between the LED and a paper ruler (Supplementary Fig. 18a). We observed that the light spread ranged from 2, 3, 4, and 5 mm at distances of 1, 2, 3, and 4 mm, respectively (Supplementary Table 3). Using basic mathematical calculations, we determined that the light dispersion angle in air was approximately 53.14° (Supplementary Note. 2). Using this dispersion angle and the optical properties of the mouse skull and tissue for red light[17,35], we performed Monte Carlo simulations to evaluate light spread within the brain[36,37]. The simulations indicated that approximately 10% of the light reached a depth of 1.25 mm and extended laterally up to 0.75 mm at a depth of 1 mm (Supplementary Fig. 18b). Hence, the estimated spatial resolution of the light when targeting ReaChR-infected neurons was approximately 0.75 mm. To avoid overlap and crosstalk between the two light sources, a minimum separation of 1.5 mm would be necessary. In our behavioral experiments, we successfully achieved the expected effects by independently stimulating the left or right cortex (left M2 or right M2). This success was likely due to a larger population of neurons responding within the targeted region. Although the spatial resolution of our LED-based system has certain limitations, clear differences in the extent of stimulation and the number of responsive cells in adjacent areas allowed for successful selective behavioral modulation.

Methods

Simulation of light distribution within the brain

To estimate the light distribution from the red LED within the brain for optical stimulation, we utilized Monte Carlo simulations (Monte Carlo eXtreme; MCX)[36,37]. In the simulation, we modeled the skull and brain tissue using a domain size of 250 × 250 × 250 with 0.1 mm voxels.

For the skull (250 x 250 x 25 of domain size), we applied an absorption coefficient of 0.6 mm^{-1}, a scattering coefficient of 2.5 mm^{-1}, an anisotropy factor of 0.92, and a refractive index of 1.36[49]. For brain tissue (250 x 250 x 225 of domain size), we used an absorption coefficient of 0.4 mm^{-1}, a scattering coefficient of 4 mm^{-1}, an anisotropy factor of 0.92, and a refractive index of 1.36[50]. These parameters were chosen to accurately represent the optical properties of both the skull and brain tissues under red light illumination.

The light source was positioned at voxel (125, 125, 0) with a dispersion angle of 53.14°. A total of 1.96×10^{17} photons·ms^{-1} were emitted from the light source, reflecting the optical power of the red LED. This setup allowed us to evaluate the light intensity and spread across the cortical regions.

Also, we have included a calculation of the divergence angles for the light spread from the LED in Added Supplementary Note 2.

Supplementary Note 2. Calculation of the divergence angles for the light spread from the LED

To calculate the angle of divergence of the LED light source used in our experimental setup, we measured the light spread by placing a paper ruler at distances ranging from 1 mm to 4 mm from the LED. This setup allowed us to measure the diameter of the range of divergence at each distance.

The angle of divergence (1) was calculated using the tangent function:

$$\tan(\alpha/2) = \frac{AW}{2AD}$$

In the equation, AW is the change in the width of the light beam, AD is the change in distance.

For example, from 1 mm to 2 mm

- Width at 1mm (W_1): 2 mm
- Width at 2mm (W_2): 3 mm
- Distance Difference (AD): 2 mm - 1 mm = 1 mm
- Width Difference (AW): 3 mm - 2 mm = 1 mm

Using the equation:

$$\tan(\alpha/2) = \frac{1}{2 \times 1} = 2^1$$

$$a = 2 \times \arctan(1/2) : 45\ 2 \times 26.57° = 53.14°$$

Also, we have included light dispersion and simulation of LED operation in Added Supplementary Figure 18:

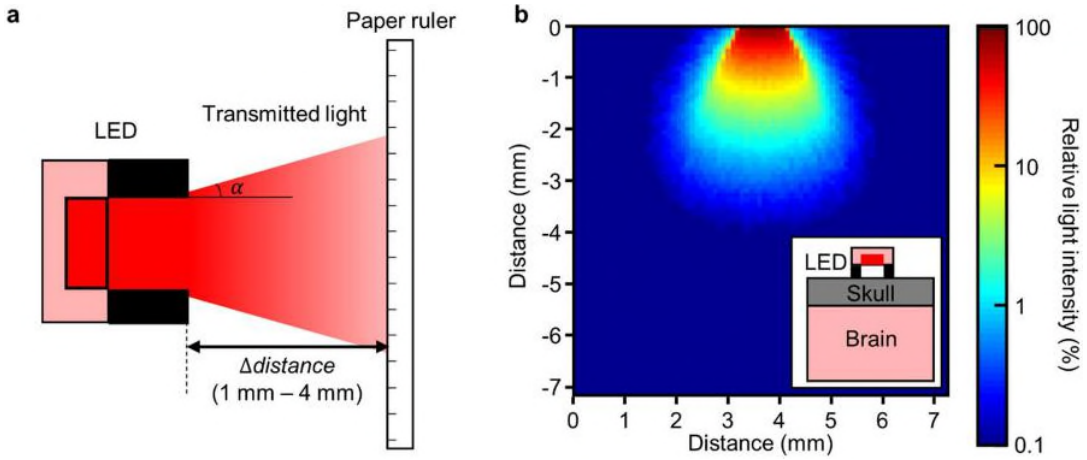

Supplementary Fig. 18: Light dispersion and simulation of LED operation. a Schematic representation of light dispersion measurement. The experimental setup used to measure the light dispersion angle (a) of the red LED. A paper ruler is positioned at varying distances (1 mm to 4 mm) from the LED to quantify the spread of transmitted light. The square piece is attached to the LED to limit the light spread. **b** Simulated light distribution within brain tissue. The Monte Carlo simulation results show the relative light intensity distribution within the brain, modeled to reflect in vivo conditions. The inset illustrates the position of the LED, skull, and brain.

6. How is the modulation pattern of 63 mW/mm^2 (red) and 275.5 mW/mm^2 (NIR) and 10Hz with ON time of 10ms (10% duty cycle) chosen? How long is the stimulation, always 10min? Are there previous experiments or literature that suggest this pattern? What is the benefit of it? This has to be clarified in the manuscript.

We appreciate the reviewer's valuable comments. The modulation pattern of 63 mW/mm^2 (red) and 275.5 mW/mm^2 (NIR) at 10 Hz with an ON time of 10 ms (10% duty cycle) was chosen based on

previous behavioral studies, such as the Open Field Test (OFT) [Park, J. et al., *Sci Adv*, 2023], preference/aversion test [Park, S. I. et al., *Proc Nat! Acad Sci U S A*, 2023], and closed-tube test [Zhou, T. et al., *Science*, 2017]. These studies typically used stimulation frequencies ranging from 5 Hz to 20 Hz. In particular, the closed-tube test demonstrated that as the stimulation frequency (5 Hz and 100 Hz) increased, the behavioral changes induced by stimulation (specifically effortful behaviors intended for winning) became more pronounced.

References:

1) Park, J. et al. A wireless, solar-powered, optoelectronic system for spatial restriction-free longterm optogenetic neuromodulations. *Sci Adv* **9**, eadi8918, doi:10.1126/sciadv.adi8918 (2023).

2) Park, S. I. et al. Stretchable multichannel antennas in soft wireless optoelectronic implants for optogenetics. *Proc Nat! Acad Sci U S A* **113**, E8169-E8177, doi:10.1073/pnas.1611769113 (2016).

3) Zhou, T. et al. History of winning remodels thalamo-PFC circuit to reinforce social dominance. *Science* **357**, 162-168, doi:10.1126/science.aak9726 (2017).

Additionally, pulse stimulation with these parameters helps reduce continuous heat buildup from the LEDs. Our temperature measurements, based on the LED's operating conditions, confirmed that pulsed stimulation kept the temperature within a safe range (Added Supplementary Fig. 6). Therefore, we set the stimulation frequency to 10 Hz (positioned within the 5-20 Hz range) and the duty cycle to 10% ensuring that the LED's temperature with the attached thermal isolator remained at a safe level to avoid brain damage. A higher duty cycle could lead to further temperature increases, resulting in potential brain damage.

Added Supplementary Figure 6

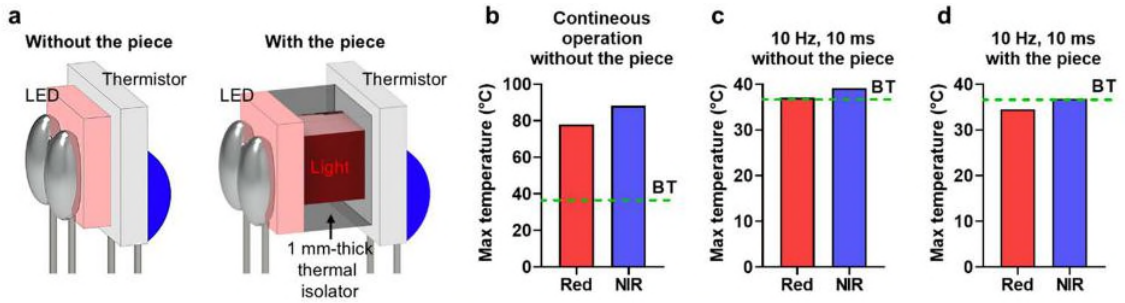

Supplementary Fig. 6: Thermal measurements of Red and NIR LEDs with and without a plastic-based thermal isolator. a Schematic of the thermal measurement setup. Illustrations showing the experimental setup used for measuring the temperature of LEDs, both with and without a 1 mm-thick thermal isolator of thermal isolator. A thermistor is attached to record temperature changes during LED operation. **b** Maximum temperature during continuous operation without the thermal isolator. **c** Maximum temperature at 10 Hz, 10 ms without the thermal isolator. **d** Maximum temperature at 10 Hz, 10 ms with the thermal isolator. In each graph, the dotted line labeled "BT" indicates the body temperature of a mouse, which is 36.6°C.

Furthermore, the duration of stimulation varied depending on the specific experiment. For example, in the circling behavior experiments, stimulation lasted for 10 minutes, whereas in the closed-tube test, it continued until the test was completed. These durations were selected based on the time frames in which experimental results were observed. Overall, our experimental conditions were sufficient to induce behavioral changes, as supported by our results.

We have added these details to the revised Results of the manuscript [lines 126-132 on page 5].

In the behavioral experiments, we primarily used a modulation pattern of 10 Hz with an ON time of 10 ms. This pattern was selected based on previous behavioral studies, including the open field test[23],

preference/aversion tests[24], and closed-tube tests[25], which commonly employ frequencies between 5 and 20 Hz to effectively induce behavioral changes. Specifically, increasing the stimulation frequency (5 and 100 Hz) in the closed-tube test led to more pronounced behavioral changes[25]. Thus, we selected 10 Hz, as it represents a midpoint within this range, balancing efficacy and minimizing heat accumulation from the LEDs.

7. The power used is very high. Have the authors checked the heat deposition in the skull and tissue? An increase in 1deg in biological tissue is already thought to be critical for neuronal behaviour, see https://www.nature.com/articles/s41593-019-0422-3 Can the authors comment on this? It would be necessary to perform measurements supported by simulations in order to exclude heat effects.

We appreciate the reviewer's concerns regarding the high power used in our study and the potential impact of heat deposition on the skull and brain tissue. We have carefully investigated this issue through experimental measurements to ensure the safety of our approach.

To mitigate heat accumulation, we operated the LEDs at a 10% duty cycle, significantly reducing continuous temperature increases. Our thermal measurements demonstrated that the maximum temperature of the LEDs during constant operation without any cooling was 77.9°C for the Red LED and 88.1°C for the NIR LED. However, with a 10% duty cycle and a small piece of plastic-based thermal isolator, the temperatures at the end of the LED dropped to 34.5°C (Red LED) and 36.8°C (NIR LED), both below body temperature.

Specifically, when comparing the conditions with and without the thermal isolator attached, operating the NIR LED at a 10% duty cycle resulted in temperatures of 36.8°C and 39.1°C, respectively. By increasing the distance between the skull surface and the LED by 1 mm, we reduced the heat transmitted to the skull to body temperature. Without this gap, the 39.1°C temperature could be directly transferred to the skull, raising the brain surface temperature exceeding 39°C, potentially leading to serious brain damage.

In conclusion, our experimental results demonstrated that tissue damage or stimulation due to heat from the LED was negligible. We have added these results and details to the revised Results [lines 158-178 on pages 6-7] and Methods [lines 530-542 on page 17].

Results

Thermal effects of LED operation

To evaluate the potential for tissue damage by heat from LED operation, we measured the surface temperature of the LEDs and estimated the corresponding temperature increase in the brain tissue (Supplementary Table 2 and Supplementary Fig. 6). During continuous operation, the LED temperature rapidly increased, reaching a maximum of 77.9°C for the Red LED and 88.1°C for the NIR LED due to overheating (Supplementary Fig. 6b). However, when operated with a 10% duty cycle, the LEDs maintained stable temperatures of 37°C for the Red LED and 39.1°C for the NIR LED, aided by adequate cooling (Supplementary Fig. 6c). In addition, we attached a plastic-based thermal isolator to limit light dispersion and measured the temperature at the end. Under the 10% duty cycle with the thermal isolator attached, during 10 minutes of operation, the maximum temperatures were 34.5°C for the Red LED and 36.8°C for the NIR LED (Supplementary Fig. 6d). These temperatures are below body temperature (37°C), indicating that the heat from the LED is unlikely to cause brain damage.

However, operating the NIR LED at 10% duty cycle without the thermal isolator resulted in temperatures exceeding 39°C, which could potentially cause brain damage[28]. Using Fourier's Law of heat conduction, we calculated the temperature change across the skull and found that the heat transferred to the brain could exceed 39°C, indicating a risk of brain damage with prolonged exposure (Supplementary Note 1).

These results suggest that under specific conditions (LED with thermal isolator, 10% duty cycle), the potential for thermal stimulation or cell damage due to LED operation is low.

Methods

Thermal measurements of LED operation

To address the potential thermal issues associated with the high-power operation of LEDs, we employed a 10% duty cycle to prevent continuous temperature increases. Thermal measurements were performed under various conditions, including constant LED operation, 10% duty cycle operation, and with and without the attachment of a plastic-based thermal isolator of thermal isolator used in the experimental setup.

A small PTC thermistor (NB-PTCO-001, Measurement Specialties) was attached to the measurement pad to monitor surface temperature (Supplementary Fig. 6a). We continuously tracked the changing resistance of the thermistor in real time and calculated the temperature using the formula provided in the datasheet. This setup enabled us to capture the maximum temperature under conditions closely mimicking the experimental setup, ensuring accurate assessments of the potential impact on brain tissue. Maximum temperature was recorded after 10 minutes of LED operation under each condition.

Also, we have included an estimation of the surface temperature of the brain caused by heat from the LED in Added Supplementary Note 1.

Supplementary Note 1. Estimation of the surface temperature of the brain caused by heat from the LED

To estimate the surface temperature of the brain caused by heat from the LED, we measured the temperature of the LED during operation.

The temperature difference (ΔT) across the skull can be calculated using:

$$\Delta T = k \times (T_{LED} - T_{brain})$$

In the equation, ΔT is the temperature difference, d is the skull thickness, and k is the thermal conductivity of the skull.

For example, if the LED temperature is 39.1°, we can estimate the surface temperature above the equation.

- Thermal conductivity of skull[6]: 0.32 W/m·K
- Skull thickness[7]: 0.25 mm
- LED temperature: 39.1°C

$$T_{brain} = T_{LED} - \Delta T = 39.1 - (39.1 - T_{brain}) \times \frac{0.00025}{0.32} = 1.0008 \approx 39.04°C$$

This LED temperature can cause severe damage to the brain[8].

Also, we have included the measurement data in Added Supplementary Table. 2.

	Resistance (Ω)	Temperature (℃)
Red, continuous operation, without the plastic-based thermal isolator	130.1	77.9
NIR, continuous operation, without the plastic-based thermal isolator	134.0	88.1

Red, 10 Hz, 10 ms (10% duty cycle), without the plastic-based thermal isolator	114.4	37.0
NIR, 10 Hz, 10 ms (10% duty cycle), without the plastic-based thermal isolator	115.2	39.1
Red, 10 Hz, 10 ms (10% duty cycle), with the plastic-based thermal isolator	113.4	34.5
NIR, 10 Hz, 10 ms (10% duty cycle), with the plastic-based thermal isolator	114.3	36.8

Supplementary Table 2: Thermal measurements of LED operation under various conditions. This table presents the resistance and corresponding temperature measurements for red and NIR LEDs under various operational conditions. The temperatures were calculated using the calculation formula provided by the provider.

$$(T) = R(0)\,x\,(1 + a\,x\,T + b\,x\,T\$)$$

where $R(T)$ is the resistance at temperature T,

(0) = 100Ω, which is the resistance at 0°C,

$a = 3.9083\,x\,10^{\%\&}$,

$b = -5.775\,x\,10^{\%(}$.

The temperature measurement includes an error margin of $\pm$ $*0.15 + 0.002\,x\,+,^{\circ}\text{-}+.$ °⁄, reflecting the precision of the thermistor.

Also, we have included the results for thermal measurements in the Added Supplementary Figure.

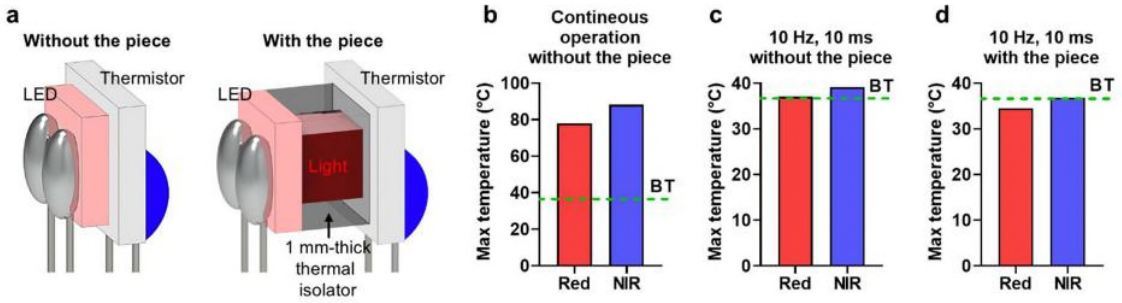

Supplementary Fig. 6: Thermal measurements of Red and NIR LEDs with and without a plastic-based thermal isolator. a Schematic of the thermal measurement setup. Illustrations showing the experimental setup used for measuring the temperature of LEDs, both with and without a 1 mm-thick thermal isolator of thermal isolator. A thermistor is attached to record temperature changes during LED operation. **b** Maximum temperature during continuous operation without the thermal isolator. **c** Maximum temperature at 10 Hz, 10 ms without the thermal isolator. **d** Maximum temperature at 10 Hz, 10 ms with the thermal isolator. In each graph, the dotted line labeled "BT" indicates the body temperature of a mouse, which is 36.6°C.

8. Red and NIR light can be used for neuromodulation without the use of genetically modified ChRs. Photobiomodulation (PBM) in order to increase neuronal activity is a growing field used to treat neurodegenerative diseases, e.g. by transcranial NIRS

https://www.frontiersin.org/journals/pharmacology/articles/10.3389/fphar.2022.965788/full

The absorption by the enzyme Cytochrome C oxidase and heat sensitive transmembrane channels is causing the effect of the PBM. This depends strongly on the wavelength (>600nm) and exposure to light (intensity, power...). The control experiments in this publication do most often not account for this possible effect. In the case of spatial resolution determination (since PBM can also increase cFos signal), this should be tested with WT mice. For motion and bahvioral contral WT mice were tested and for this certain experiment this is ok. But in the case of Parkinsonism it should be tested if the motor dysfunction of mice without genetic modification but MPTP injection can be improved by the LED probe itself without the need of optogenetics. This requires further tests.

We appreciate the reviewer's valuable suggestions and insights. Based on the feedback, we have conducted additional experiments to thoroughly investigate the potential effects of transcranial near-infrared stimulation (tNIRS) and address the specific concerns raised.

First, we accessed c-Fos expression to evaluate the effects of NIR stimulation on wild-type (WT) mice that had not been injected with viruses or upconversion particles (UCPs). We applied NIR stimulation to WT mice using the same protocol (10 Hz stimulation at 10 ms for 10 minutes) and analyzed c-Fos expression in the same target region (the striatum). The results indicated minimal c-Fos expression in response to NIR stimulation. To quantify this, we used the particle count function in the open-source software ImageJ to calculate the ratio of c-Fos-expressing cells relative to the total number of cell nuclei (DAPI). High-magnification image analysis showed that 3% of the cell in the control group (which received NIR stimulation but did not receive virus or particle injections) expressed c-FOS, compared to 9%, 15%, and 22% of cells in groups injected with 100 nL, 400 nL, and 800 nL of particles, respectively. These findings suggest that the cellular stimulation induced by tNIRS under our experimental conditions is minimal. We have included these results in the revised Methods [lines 621624 on page 19] and Results [lines 231-237 on page 8] sections, along with supplementary figures.

Methods

Additionally, to analyze the ratio of c-Fos-expressing cells relative to the total cell nuclei (DAPI), we used the particle count function in ImageJ (open-source software). Particles smaller than 5 μm were excluded from the analysis.

Results

Specifically, c-Fos expression was observed in 9%, 15%, and 22% of the total cells in the groups injected with 100, 400, and 800 nL of particles, respectively (Fig. 2c and Supplementary Figs. 11-12). In contrast, only 3% of the cells expressed c-Fos in the control group, which did not receive virus or particle injections (Fig. 2c and Supplementary Figs. 12-13). These results indicate that, under our experimental conditions, the effect of tNIRS alone was minimal, whereas the proportion of stimulated cells increased progressively with the quantity of particles injected.

Revised Figure 2

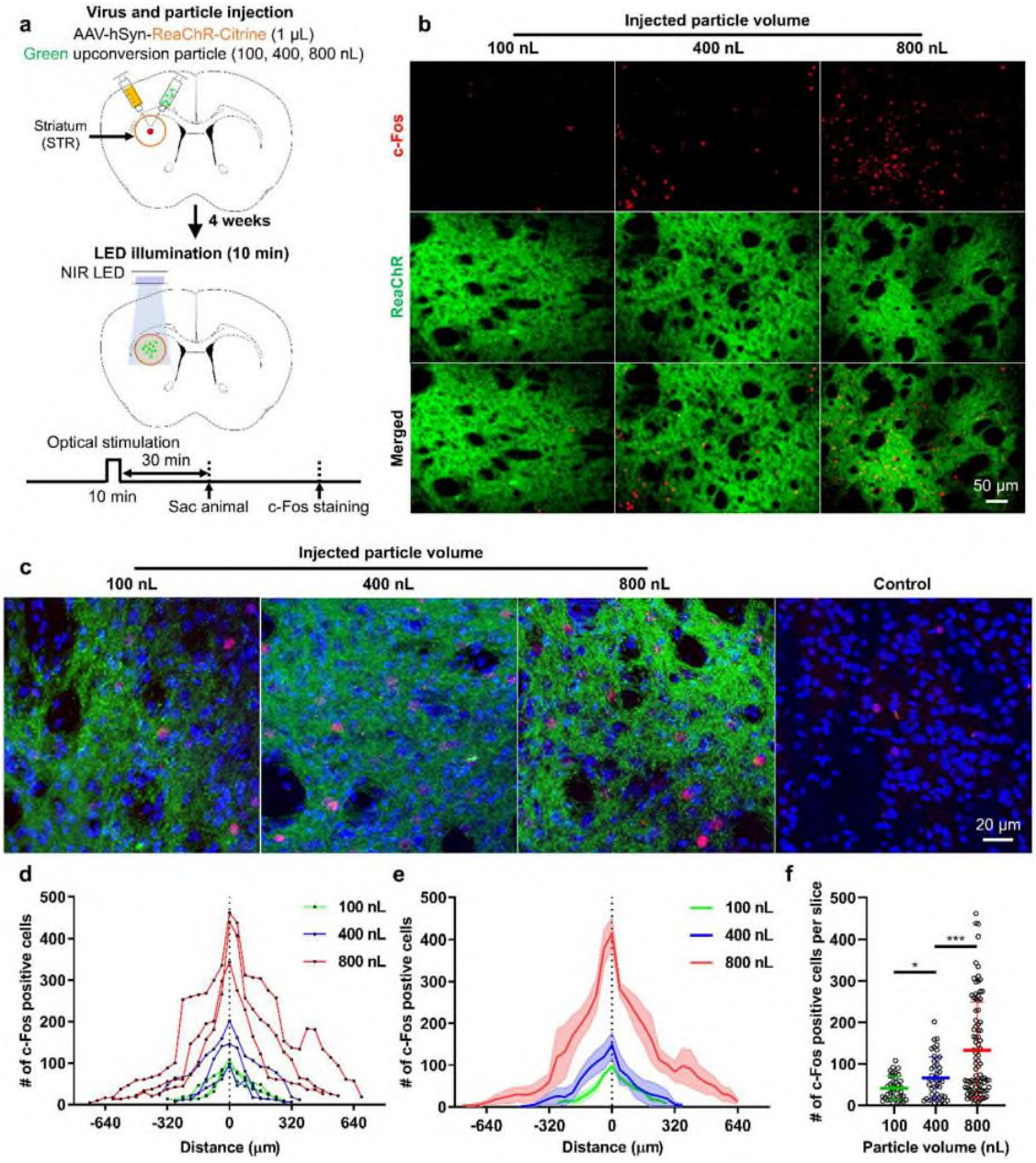

Fig. 2: Spatial resolution of transcranial brain optogenetic method in vivo. a Schematic diagrams of virus/particle injection and experimental process. ReaChR virus was injected into striatum (STR). Green upconversion particles of varying quantities (100, 400, and 800 nL at a concentration of 20 mg·mL^{-1}) were injected into the same region. After 4 weeks, the c-Fos expression experiment was conducted. **b** The expression of c-Fos in the target region according to the quantities of the particles. **c** High magnification image of c-Fos expression. The control group consists of mice that underwent NIR stimulation without any injection of virus or particles. In the image, red represents c-Fos expression, green indicates ReaChR virus-infected neurons, and blue represents DAPI (labeling cell nuclei). **d** The number of c-Fos positive cells according to the volume of particles injected into individual mice. Three mice were used for each condition. Each data point represents the number of c-Fos positive cells in a 40-μm brain slice. **e** The number of c-Fos positive cells according to the volume of particles. The bold colored lines represent the mean value from the three mice. The lighter shade represents the standard

error of the mean (SEM). **f** The number of c-Fos positive cells per slice according to the volume of particles (100 nL-400 nL: t(82)=2.616, p=0.1057445, 400 nL-800 nL: t(134)=3.708, p=0.00030456; n=39 for 100 nL; n=45 for 400 nL; n=91 for 800 nL where n is the number of slices exhibiting c-Fos expression from three mice.). Statistical analysis was performed by the two-tailed unpaired t test, and $p<0.05$ was considered significant. * $p< 0.05$, *** $p< 0.001$.

Added Supplementary Figure 11

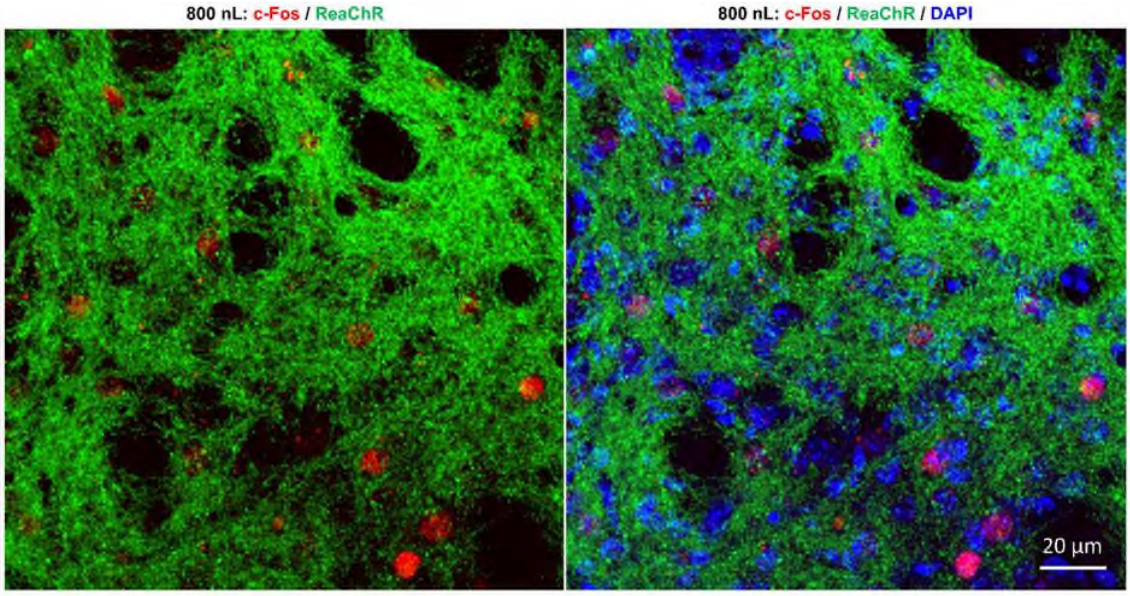

Supplementary Fig. 11: High-magnification representative confocal fluorescence images showing c-Fos expression induced by NIR stimulation in mice injected with virus and particles (800 nl). (Left) Image showing virus-infected neurons and c-Fos expression. (Right) Image showing virus-infected neurons, c-Fos expression, and DAPI staining.

Added Supplementary Figure 12

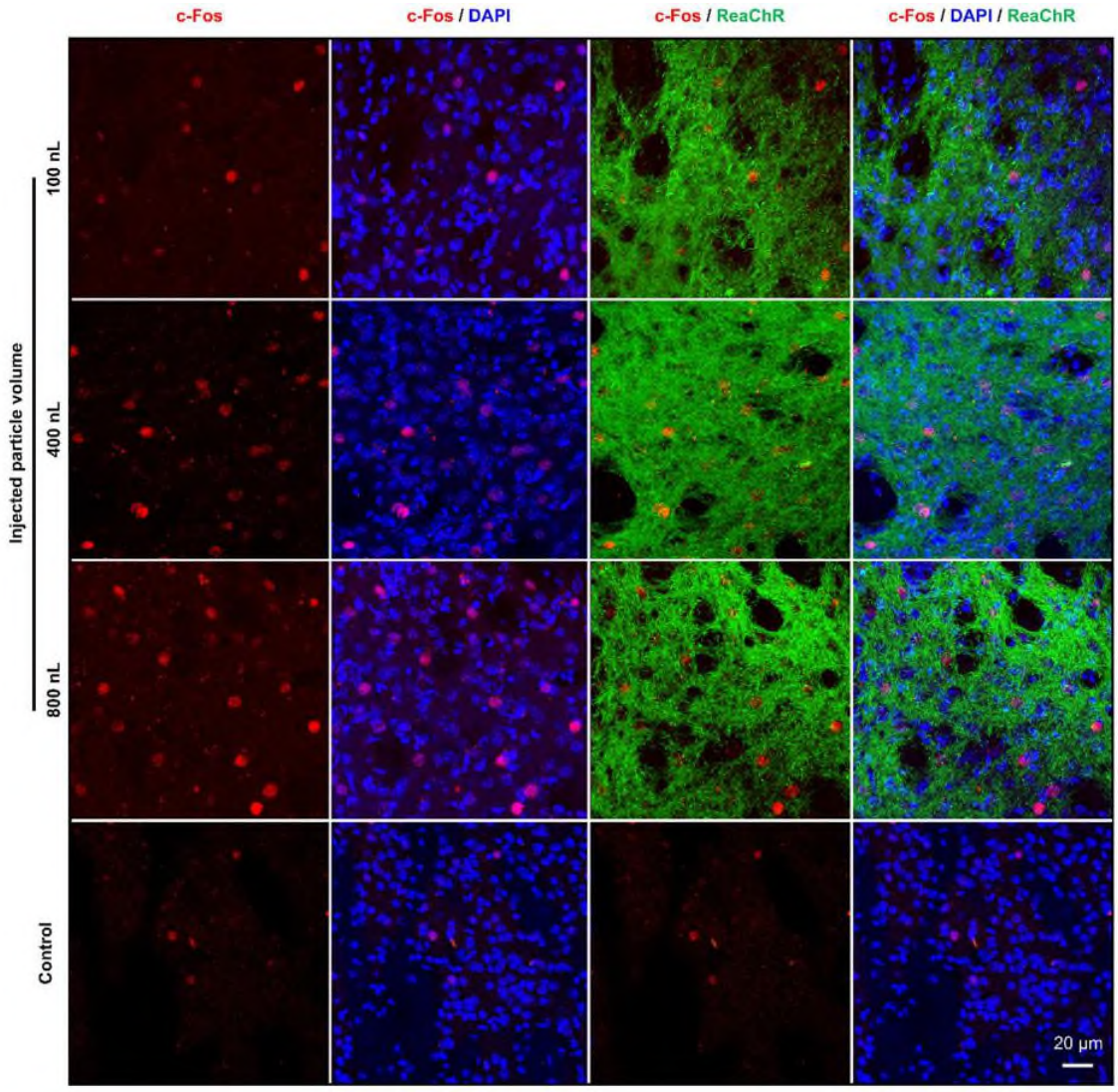

Supplementary Fig. 12: High-magnification fluorescence images showing c-Fos expression in the target region depending on the amount of particle injection. The control group represents mice that underwent NIR stimulation without the injection of both virus and particles.

Added Supplementary Figure 13

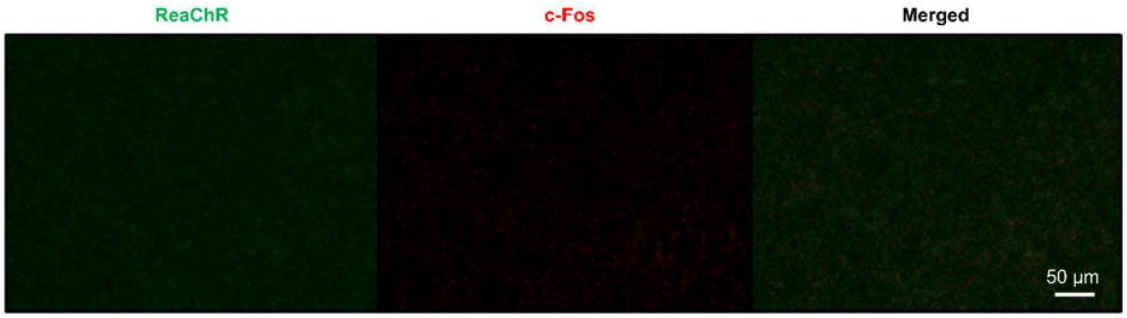

Supplementary Fig. 13: Representative confocal fluorescence image showing c-Fos expression induced by NIR stimulation in mice that were not injected with either virus or particles.

Furthermore, we investigated whether NIR stimulation could influence motor activity in MPTP-injected mice, which serve as a model for Parkinson's disease but were not genetically modified or injected with UCPs. First, we compared the activity levels between MPTP-injected mice and control mice. As expected, MPTP injection significantly reduced activity levels, consistent with Parkinson 's-like symptoms.

Next, we applied NIR stimulation using the same stimulation protocol as before, where stimulation was applied for 20 minutes with alternating 5-minute on-and-off intervals. The results showed that NIR stimulation did not lead to any significant increase in activity levels in the MPTP-injected mice, which were not treated with viruses or UCPs. This suggests that the behavioral changes observed in our original experiments were due to optogenetic modulation rather than any potential effect from PBM.

These findings indicate that under our experimental conditions (NIR stimulation at 275.5 mW/mm^2 within 10 minutes, etc.), tNIRS or PBM has no significant effect on neural activity or behavior in the absence of genetic modifications. We have included these additional experimental results in the revised Results [lines 399-406 on page 13] and added supplementary figures.

As a control experiment, we investigated whether NIR stimulation could affect motor activity in MPTP-injected mice (a Parkinson's disease model) without genetic modifications or UCPs. MPTP injection significantly reduced the activity levels (Supplementary Movie 10 and Supplementary Figs. 25a-b), and NIR stimulation, applied using the same protocol, did not lead to increased activity in these mice (Supplementary Movie 11, Supplementary Figs. 25c-e, and Supplementary Fig. 26). These results suggested that the improvements observed in our experiments were specifically attributable to optogenetic modulation.

Added Supplementary Figure 25

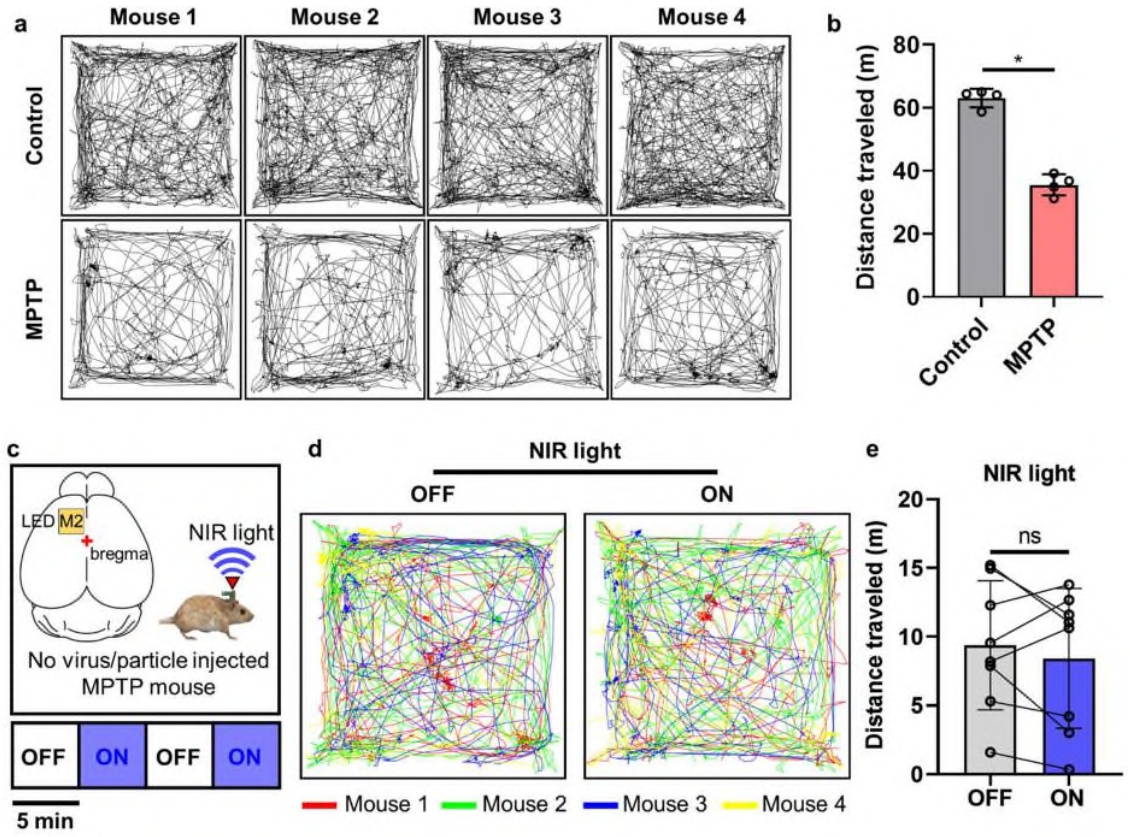

Supplementary Fig. 25: Effects of MPTP Injection and NIR Light on locomotor activity in mice. a Trajectories of each intact and MPTP-injected mouse for 20 min. **b** Comparison of the distance traveled for 20 min by intact and MPTP-injected mice (p=0.0286, white circle: n=4 where n is the number of mice.). **c** Schematic illustration showing the experimental process. The inset displays the LED placement on the M2 region of the brain. Testing for light delivery consisted of two cycles. One cycle consisted of two 5 min epochs with alternating light delivery (OFF-ON). We operated the system with a 10 Hz frequency and a 10 ms ON time during stimulation. **d** Trajectories of each mouse according to NIR LED on and off on the M2 region. The color of the line represents each mouse. **e** Comparison of the distance traveled according to red LED on and off on the M2 region (p=0.4609, white circle: n=8 for all data, where n is the number of cycles). The data are presented as mean values +/− s.d. with individual data points. Statistical analysis was performed by the two-tailed Mann-Whitney test (Supplementary Fig. 21b) and the Wilcoxon matched-pairs signed rank two-tailed test (Supplementary Fig. 21e). $p<0.05$ was considered significant. ns: no statistical significance.

Added Supplementary Figure 26

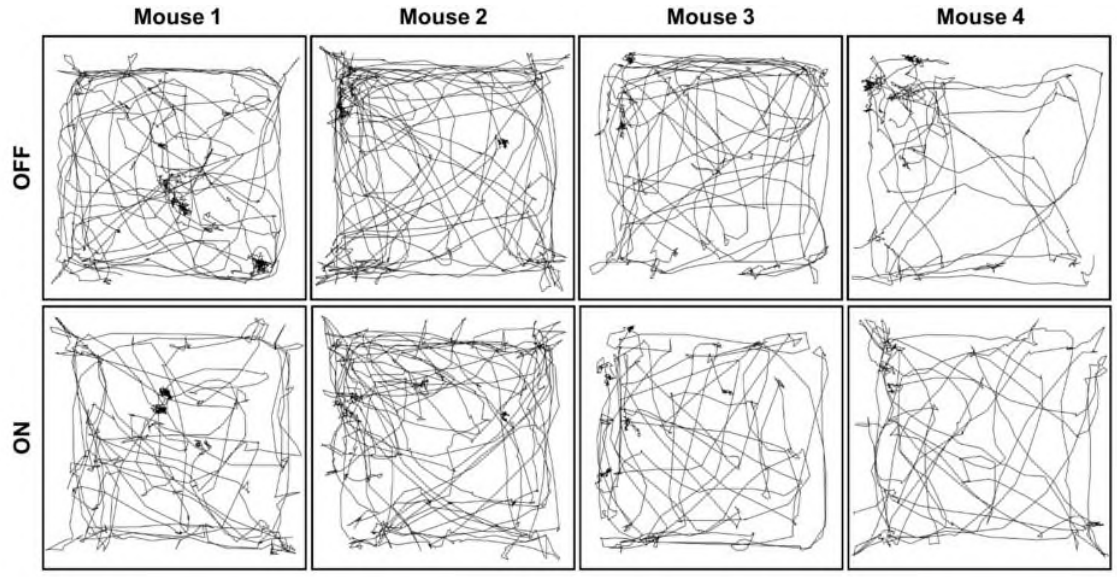

Supplementary Fig. 26: Movement trajectories of mice in open field tests with NIR stimulation. Trajectories of each mouse according to NIR LED on and off on the M2 region. We operated the system with a 10 Hz frequency and a 10 ms ON time during stimulation.

9. It is not clear if the position of the LED probe in the control experiments mentioned in l. 195 is exactly the same as in the experiment later. Where is it placed? This should be added in a figure.

We apologize for the missing information and appreciate the reviewer's valuable feedback. As suggested, we have included a figure showing the exact position of the LED probe on the brain's surface. This figure ensures clarity and consistency in the methodology by illustrating the precise position.

We have updated the manuscript to include this revised supplementary figure and added the information in the revised Results [lines 259-263 on page 9].

After attaching the LED array to the skull above the left premotor cortex (M2) region, we observed the behavioral activity of the mice in response to the LED in the ON and OFF states in an open-field maze (as described in the Methods section). We found no differences in behavioral activity during the red and NIR LED on- and off-states (Supplementary Movie 2 and Supplementary Fig. 15).

Added Supplementary Figure 15

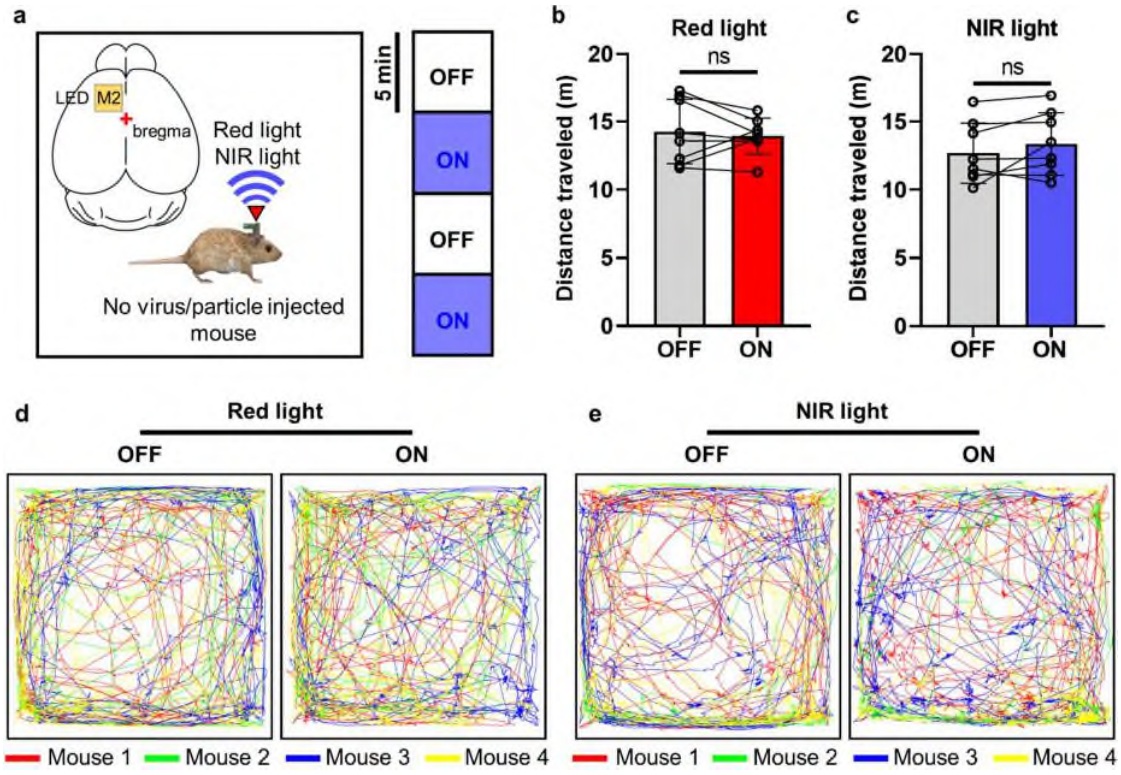

Supplementary Fig. 15: Effect of light delivery into the brain using the optoelectronic system on general locomotor activity. a Schematic illustration showing the experimental process. The inset displays the LED placement on the M2 region of the brain. Testing for light delivery consisted of two cycles. One cycle consisted of two 5 min epochs with alternating light delivery (OFF-ON). We operated the system with a 10 Hz frequency and a 10 ms ON time during stimulation. **b** Comparison of the distance traveled according to red LED on and off ($t(7)=0.5515$, $p=0.5985$). **c** Comparison of the distance traveled according to NIR LED on and off ($t(7)=1.459$, $p=0.1879$). **d** Trajectories of each mouse according to red LED on and off. The color of the line represents each mouse. **e** Trajectories of each mouse according to NIR LED on and off. The color of the line represents each mouse. The data are presented as mean values +/− s.d. with individual data points (white circle: n=8 for all data, n is the number of cycles. This experiment was conducted with four mice.). All statistical analyses were performed by the two-tailed Paired t test, and $p<0.05$ was considered significant. ns: no statistical significance.

10. The wording of mind and body control is misleading and should be named into behavioural and motion control instead.

We appreciate the reviewer's valuable suggestion regarding the terminology used in our study. We agree that the terms "mind control" and "body control" could be misleading and do not accurately represent the nature of our experiments. Following the reviewer's advice, we have revised the manuscript to use "behavioral control" and "motion control" instead.

These changes have been implemented throughout the manuscript.

11. The improvement in resolution should be compared to the resolution of the mentioned transcranial techniques, numbers should be provided.

We appreciate the reviewer's valuable suggestion. As advised, we have included a numerical comparison of the temporal and spatial resolutions between our technique and the transcranial techniques mentioned [Yang, D. et al., ***Front Neurosci***, 2021 and Mosilhy, E. A. et al., ***Life Sci***, 2022]. The temporal resolution for the other techniques was referenced from previous studies, while the temporal resolution of our technique follows optogenetics standards [Yang, D. et al., ***Front Neurosci***, 2021 and Mosilhy, E. A. et al., ***Life Sci***, 2022]. The spatial resolution was determined from our experimental results (0.5 mm stimulation range observed in c-fos results) and previous results on transcranial optogenetics with high-sensitive opsins without UCPs (0.8 – 1 mm stimulation range) [Chen, R. et al., ***Nat Biotechnol***, 2021]. These comparisons have been added in a supplementary figure in the revised supplementary information.

References:

1) Yang, D., Shin, Y. I. & Hong, K. S. Systemic Review on Transcranial Electrical Stimulation Parameters and EEG/fNIRS Features for Brain Diseases. Front Neurosci 15, 629323, doi:10.3389/fnins.2021.629323 (2021).

2) Mosilhy, E. A. et al. Non-invasive transcranial brain modulation for neurological disorders treatment: A narrative review. Life Sci 307, 120869, doi:10.1016/j.lfs.2022.120869 (2022).

3) Chen, R. et al. Deep brain optogenetics without intracranial surgery. Nat Biotechnol 39, 161-164, doi:10.1038/s41587-020-0679-9 (2021).

Added Supplementary Figure 14

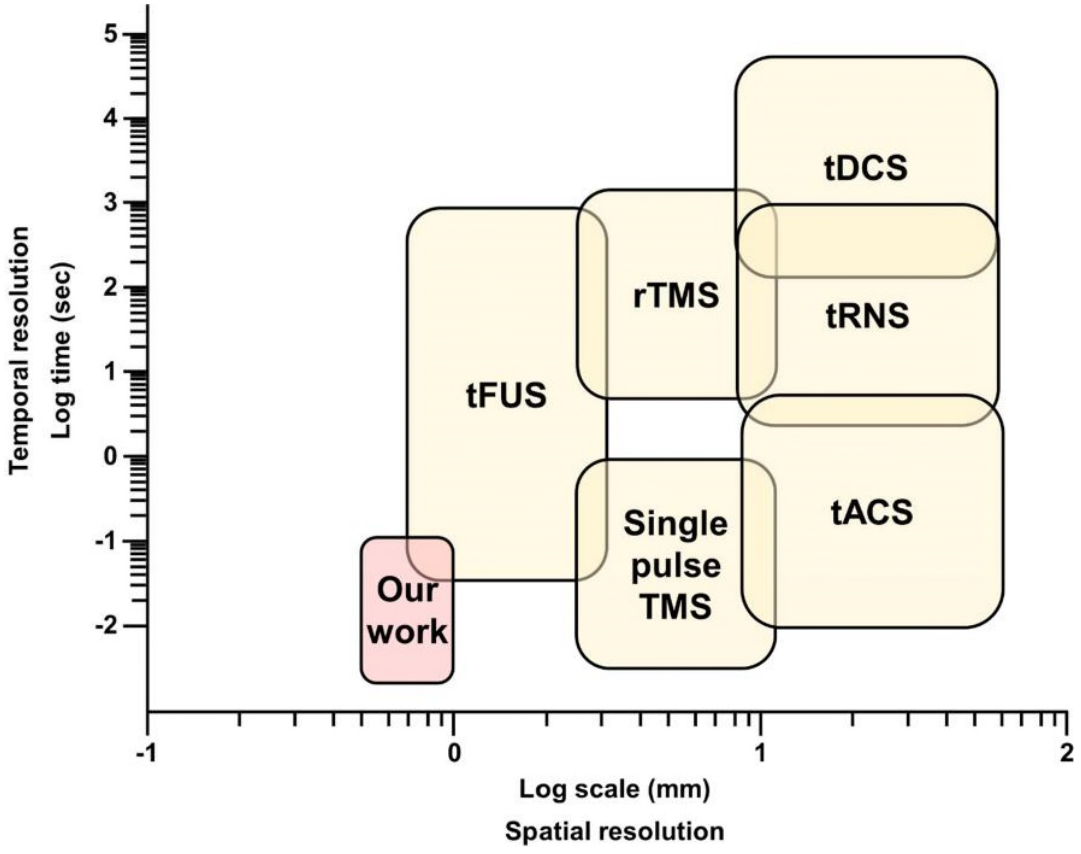

Supplementary Fig. 14: Comparison of temporal and spatial resolution in transcranial brain stimulation techniques[4,5]**.** Our work (pink shaded area) demonstrates higher spatial resolution

(approximately 0.5 mm) compared to traditional non-invasive methods such as transcranial focused ultrasound stimulation (tFUS), repetitive transcranial magnetic stimulation (rTMS), transcranial direct current stimulation (tDCS), transcranial alternating current stimulation (tACS), transcranial random noise stimulation (tRNS), and single-pulse transcranial magnetic stimulation (single pulse TMS). The temporal and spatial resolutions are plotted on a logarithmic scale, highlighting the enhanced precision of our transcranial optogenetic neuromodulation approach for targeting specific brain regions effectively.

Also, we have revised the manuscript to include these numerical comparisons in the revised Results [lines 244-249 on pages 8-9].

Importantly, the spatial resolution achieved using our technique (approximately 0.5 mm) exceeds the roughly 1 mm resolution offered by transcranial focused ultrasound stimulation (tFUS), which was previously considered the most precise transcranial brain stimulation method (Supplementary Fig. 14)[29]31. Additionally, the spatial resolution of our technique surpasses that attained by transcranial optogenetics (approximately 1 mm) using only high-sensitivity opsin[10].

We appreciate the reviewer's valuable comments again and believe our manuscript has improved significantly as a result.

RESPONSES TO REVIEWER'S COMMENTS FOR NCOMMS-23-12932C

We appreciate the reviewer's careful evaluations and insightful comments on our paper. We have addressed all the comments and feel that the constructive comments were in many ways helpful and significantly improved our manuscript. We have listed each of the reviewers' comments, followed by our responses in blue, and a marked-up version of a revised manuscript with changes highlighted in yellow.

Reviewer Comments:

Reviewer #1

The authors have addressed all the Reviewers' comments accordingly. I suggest the paper be accepted.

Thank you for your positive feedback and recommendation. We appreciate the review process and are grateful for the constructive comments that helped improve our manuscript.

Reviewer #2

The authors have thoroughly and thoughtfully addressed my previous comments on their manuscript. The in-depth elaboration on the device's thermal and spectral properties, along with the additional information on control experiments, provides essential and valuable insights into their work and findings. These enhancements strengthen both the experimental setup and analysis, making the experimental approach and the concept of this transcranial LED-based stimulation device clearer and more accessible. Looking forward, an overlap of 60% between blue UCPs and ReaChR may be excessive and could potentially reduce effectiveness when aiming to inhibit neurons through stGtACR2.

There is one remaining concern which should be addressed before the publication:
Line 301: The authors simulate and calculate the optimal distance for LEDs within the device, yet the actual LED spacing on the skull remains unclear. The authors should specify the precise placement for the different experiments (e.g., motion control and behavioral studies), including details on the distances of the LEDs and the accuracy of the placement in order to guarantee reproducibilty.

We appreciate the reviewer's valuable feedback regarding the placement and arrangement of LEDs in our experiments. To address the reviewer's concern and ensure reproducibility, we have provided detailed information on the specific LED positioning used in each experimental setup. For the motion control experiments, the two LEDs were placed closely side by side to allow direct, localized stimulation of adjacent areas, facilitating precise motion control measurements. In the behavioral control experiments, we positioned the LEDs facing each other at a 30-degree angle to enable simultaneous light delivery to a single target region, ensuring effective stimulation within the intended behavioral area.

Additionally, in experiments where only activation or inhibition was applied independently to separate regions, each LED was positioned directly above the respective target area to deliver light perpendicularly onto the skull. This setup ensured precise stimulation of the intended area while minimizing off-target effects. These configurations have been added to the revised Methods section, providing clarity on LED placement for reproducibility across similar studies.

We have added the following statements in the revised Methods [lines 584-601 on pages 18-19].

In the motion control experiment, we injected the ReaChR virus into the left/right premotor cortex (+1.1; ± 0.6; −1.25, AP; ML; DV, in millimeters from the bregma) and superior colliculus (-4; −0.75; −1.1, AP; ML; DV, in millimeters from the bregma) regions, respectively. We only

injected the green-emitting UCPs into the superior colliculus region. For this setup, the two LEDs were placed closely side by side to enable localized, direct stimulation of adjacent regions, enhancing motion control precision.

In the behavioral control and food competition experiments, we injected ReaChR and stGtACR2 viruses and blue-emitting UCPs particles into the medial prefrontal cortex region (+2.6; +0.12; −1.5, AP; ML; DV, in millimeters from the bregma). To enable effective simultaneous stimulation, the LEDs were positioned facing each other at approximately a 30-degree angle, ensuring consistent light delivery to the target behavioral area.

In the behavioral experiment using Parkinson's disease-induced mice, we injected ReaChR virus into the premotor cortex region (+1.1; −0.6; −1.25, AP; ML; DV, in millimeters from the bregma) and green-emitting UCPs into the dorsomedial striatum region (+0.5; −1.5; −3.2, AP; ML; DV, in millimeters from the bregma).

Additionally, in experiments where only activation or inhibition was applied independently to separate regions, each LED was positioned directly above the respective target area to deliver light perpendicularly onto the skull.

Thank you for your thoughtful and encouraging feedback. We appreciate your insights and are grateful for your support in strengthening our manuscript.